Tuned Pulse Sound Source Characterization in Gulf of Mexico

JASCO Applied Sciences (USA) Inc.

19 December 2023

Submitted to:

Marc Rocke

TGS

Work Order signed 28 August 2023

Authors:

S. Bruce Martin
Carmen B. Lawrence
Julien J.-Y. Delarue
Colleen C. Wilson

P001753-001
Document 03240
Version 1.0

JASCO APPLIED SCIENCES

Suggested citation:

Martin, S.B., C.B. Lawrence, J.J.-Y. Delarue, and C.C. Wilson. 2023. Tuned Pulse Sound Source Characterization in Gulf of Mexico. Document 03240, Version 1.0. Technical report by JASCO Applied Sciences for TGS.

Report approved by:

Version	*Role*	*Name*	*Date*
1.0	Project Manager	Mark Cotter	18 December 2023
	Senior Scientific Reviewer	David Hannay	18 December 2023

Disclaimer: The results presented herein are relevant within the specific context described in this report. They could be misinterpreted if not considered in the light of all the information contained in this report. Accordingly, if information from this report is used in documents released to the public or to regulatory bodies, such documents must clearly cite the original report, which shall be made readily available to the recipients in integral and unedited form.

Authorship statement: Individual authors of this report may have only contributed to portions of the document and thus not be responsible for the entire content. This report may contain standardized (boilerplate) components that are common property of JASCO and are not directly attributed to their original authors/creators. The entire content of this report has been subject to senior scientific review by the qualified person listed in the front matter of the document.

Contents

Executive Summary 1
1. Introduction 2
2. Methods 5
2.1. Measured Sound Sources 5
2.2. Acoustic Data Acquisition 7
2.2.1. Underwater Acoustic Recorders 7
2.2.2. Deployment Locations 8
2.2.3. Mooring Design 9
2.2.4. Acoustic Data Analysis 12
3. Results 16
3.1. Total Sound Levels 16
3.2. Received Levels from the Pulsed Sources 16
3.3. Cumulative Sound Exposure Levels 20
3.4. Behavioral Disturbance 21
3.5. Masking of Biologically Relevant Sounds 24
3.6. Marine Mammal Detections and Exposure 27
3.6.1. Detector Performance 27
3.6.2. Sperm Whales 27
3.6.3. Delphinids 29
4. Discussion and Conclusion 31
4.1. Background Noise Levels 31
4.2. Measurement Depth Considerations 31
4.3. Comparison of the Effects of Sound from the Tuned Pulsed Source and Airgun Arrays 35
4.4. Marine Mammals 36
4.4.1. Sperm Whales 36
4.4.2. Delphinids 36
Literature Cited 38
Appendix A. Recorder Calibration and Mooring Design A-1
Appendix B. Acoustic Data Analysis B-1
Appendix C. Marine Mammal Detection Methodology C-1

Figures

Figure 1. General location of the tuned pulse source (TPS) evaluation during an ocean bottom node (OBN) survey already being conducted by TGS for Shell. 2
Figure 2. (Left) Time domain and (right) spectra modelled signatures of an ultra low-frequency (ULF; 140,000 in^3), and a very-low-frequency (VLF; 30,000 in^3) configuration of the TPS compared to a 3 × 2 × 5.74 L airgun array (6 airguns at 350 in^3 each; 2100 in^3). 3
Figure 3. Configuration of the 5000 in^3 standard seismic array used for comparison to the TPS. 5
Figure 4. Track lines of the *Sanco Sword* during the airgun array exposures. 6
Figure 5. Bathymetry of the project area. 7
Figure 6. JASCO AMAR G4 in anodized aluminum housing 8
Figure 7. Deployment location of each AMAR showing depth contours. 8
Figure 8. Vessel *Marianne G* was used for deployment and retrieval operations. 9
Figure 9. Mooring design employed for the TGS measurements. 10
Figure 10. Model of the long mooring assuming 0.6 m/s of currents 11
Figure 11. Total sound level summary from station 5145 16
Figure 12. Comparison of the received levels from (top) the dual TPS pass versus (bottom) the airgun array pass, at the closest points of approach (CPA) to station 5145 17
Figure 13. Peak sound pressure level (PK) as a function of distance to the source using data recorder 5145. 18
Figure 14. Peak sound pressure levels (PK) as a function of direction to the vessel from Station 5145. 18
Figure 15. Per pulse auditory frequency weighted sound exposure levels for all detected pulses as a function of absolute value of the distance to the source type 19
Figure 16. Pulse duration versus range by source type. Positive and negative values on the x-axis show distances to the north and south of the recorder, respectively. 19
Figure 17. Cumulative marine mammal weighted sound exposure levels for each of the stations and source types. 20
Figure 18. Received per-pulse M-Weighted sound pressure levels as a function of the source and distance from Station 5145 to the sources. Positive and negative values on the x-axis show distances to the north and south of the recorder, respectively. 22
Figure 19. Available Listening Range (100 % is good) at Station 5145 for Rice's whale 80 Hz downsweeps. Negative distances are south of the recorder, positive distances to its north. 25
Figure 20. Available Listening Range (100 % is good) at Station 5145 for dolphin whistles at 10000 Hz. Negative distances are south of the recorder, positive distances to its north. 26
Figure 21. Sperm whale click trains: Spectrogram of click trains recorded at Stn 5129 on 1 Sep 2023 27
Figure 22. Sperm whale occurrence 28
Figure 23. Sperm whale: Number of hours per day containing manual detections at Stn 5129 and Stn 5145. 28
Figure 24. Unidentified dolphin: Spectrogram of unidentified dolphin whistles and click trains recorded at Stn 5145 on 6 Sep 2023 29
Figure 25. Unidentified dolphin whistle occurrence 29
Figure 26. Unidentified dolphin click occurrence 30
Figure 27. Dolphins: Number of hours per day containing unidentified manual detections (both whistles and clicks) at Stn 5129 and Stn 5145. 30
Figure 28. Photo of rope with hairy fairings embedded. 31

Figure 29. Top-down view of the per-pulse broadband SPL from the 5000 in3 array. Higher sound levels are emitted horizontally at endfire than broadside. From the Gundalf report Gundalf_repC_5000_8m_24331.pdf. 32
Figure 30. Range-depth cross-sectional view of the per-pulse broadband SPL from the 5000 in3 array. Higher sound levels are emitted downwards. From the Gundalf report Gundalf_repC_5000_8m_24331.pdf 33
Figure 31. Beampattern sampling for a sound source near the surface following the walkaway pattern shown in (A). The samples from a hydrophone at 100 m depth are shown at (B), at 1000 m at (C) and combining both at (D). In these figures, 0 degrees azimuth is forward endfire, 90 degrees is broadside and 180 is aft endfire. Zero degrees elevation is the sea surface and 90 is the seabed. White cells are not sampled by the vessel tracks. 34
Figure A-1. Split view of a G.R.A.S. 42AC pistonphone calibrator with an M36 hydrophone. A-1
Figure B-1. Typical geometry of sound source characterization (SSC) measurements and the associated terminology used in this report. B-1
Figure B-2. Decidecade frequency bands (vertical lines) shown on (top) a linear frequency scale and (bottom) a logarithmic scale. B-4
Figure B-3. Sound pressure spectral density levels and the corresponding decidecade band sound pressure levels of example ambient sound shown on a logarithmic frequency scale. B-5
Figure B-4. Auditory weighting functions for the functional marine mammal hearing groups as recommended by Southall (2019). B-7
Figure B-5. Auditory weighting functions for the functional marine mammal hearing groups as recommended by Southall et al. (2007). B-8
Figure C-1. Flowchart of the automated click detector/classifier process. C-2
Figure C-2. Flowchart of the click train automated detector/classifier process. C-3
Figure C-3. Illustration of the contour detection process. C-4
Figure C-4. Illustration of the search area used to connect spectrogram bins. C-5
Figure C-5. The Automated Data Selection for Validation (ADSV) process. C-7

Tables

Table 1. Peak sound pressure level (PK; dB re 1 µPa), and sound exposure level (SEL; dB re 1 µPa^2 s) thresholds for, auditory injury (PTS onset), and TTS onset for marine mammals for impulsive sounds, as recommended by NMFS (2018). 4
Table 2. Wood et al. (2012) acoustic sound pressure level (SPL) thresholds used to evaluate potential behavioral impacts to marine mammals. 4
Table 3. Description of measurement locations. 8
Table 4. Auditory frequency weighted cumulative sound exposure levels for each source and station. 21
Table 5. Linear model fit parameters for the per-pulse SPLs in Figure 18 (weighted by the Southall et al (2007) M-weighting), to the equation $SPL = A + B\log 10R$, where R is the distance to the vessel (100–15000 m), *A* is the effective source level, and *B* is the effective geometric spreading coefficient. Note that these values are only valid for the location and sources measured, as evidenced by the substantial differences between the shallow (north of recorder) and deep (south of recorder) parameters. 23
Table 6. Distances (m) to the Wood et al (2012) SPL thresholds for behavioral disturbance for species or groups that could occur in the project area (see Table 2). SPLs are M-weighted (Southall et al 2007). Distances were computed by finding the distance at which the linear equations from Table 5 fall below the disturbance thresholds. The maximum distance computed was 20000 m to avoid extrapolating far beyond the maximum distances measured. 23

Table 7. Decidecade bands analyzed for the Available Listening Range. 26
Table 8. Automated detector performance 27
Table B-1. Decidecade band center and limiting frequencies (Hz). B-5
Table B-2. Decade band center and limiting frequencies (Hz). B-6
Table B-3. Parameters for the auditory weighting functions recommended by Southall et al (2019). B-6
Table B-4. Parameters for the auditory weighting functions recommended by Southall et al. (2007). B-8
Table C-1. List of automated detectors used to identify clicks produced by odontocetes. C-3
Table C-2. Fast Fourier Transform (FFT) and detection window settings for all automated contour-based detectors used to detect tonal vocalizations of marine mammal species expected in the data. C-5
Table C-3. A sample of automated detector classification definitions for the tonal vocalizations of cetacean species expected in the area. C-6

Executive Summary

JASCO Applied Sciences (JASCO) was contracted by TGS to undertake a sound source characterization (SSC) study of the tuned pulse source (TPS) in the Gulf of Mexico from 31 August to 7 September 2023. The SSC involved collecting and analyzing data and interpreting the results, focusing on understanding potential impacts on marine mammals. The scope of the study was to determine the relative sound levels of the TPS within the hearing bands of marine mammals compared to standard airgun surveys. Data were collected using a walk-away pattern that sampled the endfire sound levels from 17500 m north of the recorders to 20000 m south. Broadside lines 5 km long were run with offsets of 170, 670, 1920 and 3920 m. Three sources were measured – a 5000 in^3 airgun array, a 28000 in^3 TPS and a dual 28000 in^3 TPS configuration. Each source fired once every 60 seconds.

The source characterization hydrophones were deployed on long-line moorings to sample at a depth of ~100 m. The water depth at the deployment site was 450 m. The start of the measurement lines to the 17500 m north of the recorders were in ~200 m water depth while the end of the lines 20000 m to the south were at ~900 m. Data were successfully collected from both recorders, however, they had very high levels of current induced movement noise that affected the ability to assess behavioral disturbance and masking from one of the recorders. The data from the other were suitable for these metrics. Measured sound levels when the source and vessels were to the north of the recorders were 5–10 dB higher than when they were to the south. This demonstrates the need to include the acoustic propagation environment in the predication and interpretation of sound levels in complex environments.

Sperm whales were present near both recorders almost daily during the recording period. Delphinid vocalizations were detected every day of the recording period. Both were detected more commonly outside of active source times. This suggests that their sounds may have been masked, changes in their vocalization behavior may have occurred, or the animals avoided the area when sources were active.

This trial allowed for a direct comparison of the received sound levels of a typical airgun array (5000 in^3), with a single or dual tuned pulse source. Assuming the seismic imaging quality of the sources is comparable, the TPS is strongly preferred from a marine mammal sound exposure viewpoint. The sound exposure levels produced by dual TPS were 10–14 dB lower for LF mammals, and 28–29 dB lower for HF and VHF mammals. This equates to at least a 3-fold reduction in exposure distance and 9-fold decrease in exposure area for LF mammals. For the HF and VHF mammals, the distances are reduced by a factor of 25 and the area by a factor of 625.

With respect to distances for behavioral disturbance, the shallow water yielded substantially longer disturbance distances in most cases. The distances at which 50 % of the individuals of sensitive species are likely to be disturbed were 5–20 km, while those distances were 1.1 km or less for the less sensitive species such as dolphins and sperm whales. In all cases the distances for the airguns were at least double those for the dual TPS, and the dual TPS distances were greater than for the single TPS.

The percentage of the normal available listening range (ALR) for marine mammals was computed as an index of communication masking. Since seismic pulses are known to reverberate, the amount of time after a pulse that is masked is of interest. The ALR was reduced for 1–2 seconds after the pulse when the source as up to 10 km away, compared to ~5 seconds for the airgun arrays. Substantial masking was found due to the tow vessel. The vessel sounds would cause substantial masking within 5 km for the 80 Hz downsweep of Rice's whales and within ~2 km for the dolphin whistles. Those distance are longer in shallow water than deep.

1. Introduction

JASCO Applied Sciences (JASCO) was contracted by TGS to undertake a sound source characterization (SSC) study of the tuned pulse source (TPS) in the Gulf of Mexico in September 2023. The SSC involved collecting and analyzing data and interpreting the results, focusing on understanding potential impacts on marine mammals. The scope of the study was to determine the relative sound levels of the TPS within the hearing bands of marine mammals compared to standard airgun surveys.

TGS conducted the survey in the Gulf of Mexico (Figure 1) from 31 August to 7 September 2023. Two calibrated Autonomous Multichannel Acoustic Recorders (AMARs) were deployed to measure sound levels produced by the survey.

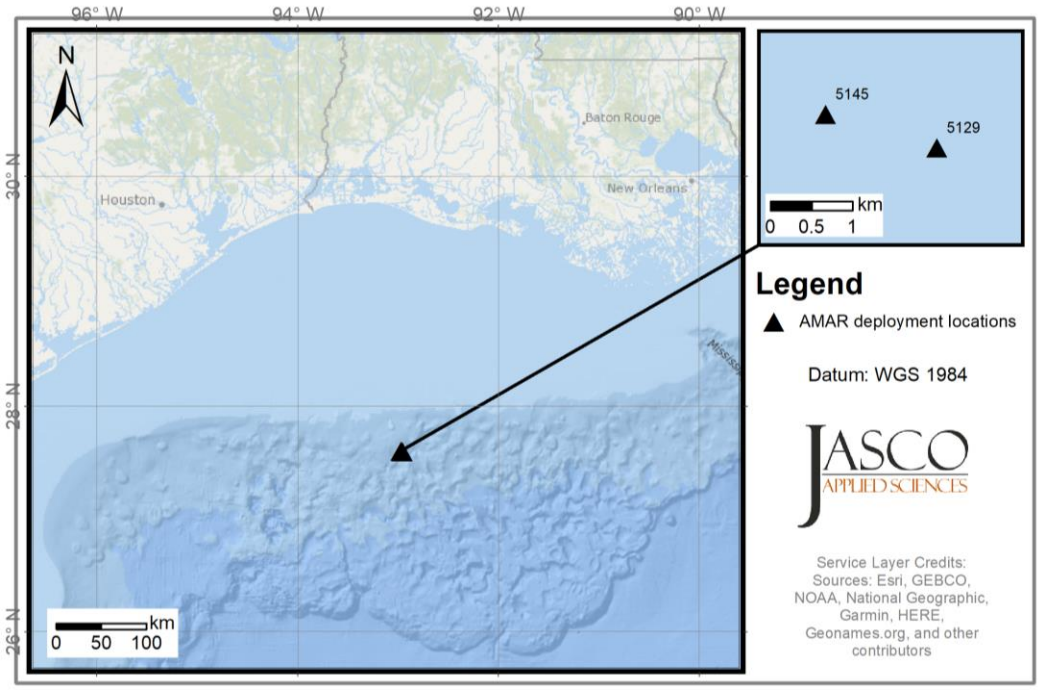

Figure 1. General location of the tuned pulse source (TPS) evaluation during an ocean bottom node (OBN) survey already being conducted by TGS for Shell.

The TPS is a variation on a standard airgun. It uses a much larger volume and lower air pressure. The larger volume lowers the primary frequency of the bubble pulse, while the lower pressure reduces the high frequency content (Chelminski et al. 2019). These changes have two benefits. First, the lower primary frequency penetrates farther into the seabed and thus yields better images of the deep strata. Second, the reduced high frequencies should reduce the sound exposure of marine mammals to seismic surveys that employ TPSs rather than standard airgun arrays. The hearing sensitivity of marine mammals is represented by their auditory frequency response functions (see Appendix B.4). Three mammal hearing groups occur in the Gulf of Mexico: low-frequency (LF) cetaceans (e.g., Rice's whale), mid-frequency (MF) cetaceans (sperm, killer, and pilot whales as well as beaked whales and most dolphins), and high-frequency (HF) cetaceans (dwarf and pygmy sperm whales). The mid-frequency animals are by far the most common. These groups have substantially reduced hearing sensitivity at low frequencies; therefore, reducing the high-frequency content of the source will likely decrease any effects on marine mammals. The purpose of the current study is to provide an in situ measurement of the difference between a standard airgun array and a single or dual 28000 in^3 TPS.

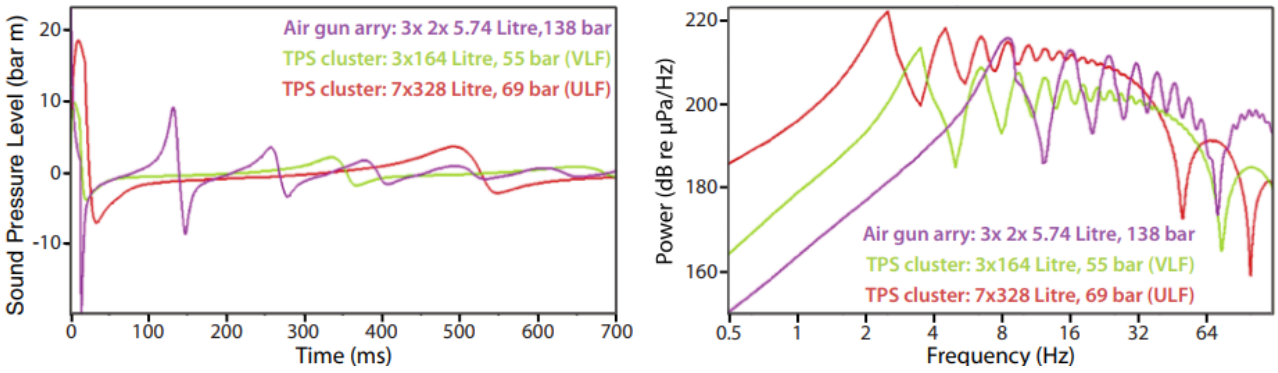

Figure 2. (Left) Time domain and (right) spectra modelled signatures of an ultra low-frequency (ULF; 140,000 in^3), and a very-low-frequency (VLF; 30,000 in^3) configuration of the TPS compared to a 3 × 2 × 5.74 L airgun array (6 airguns at 350 in^3 each; 2100 in^3). Figure 3 from Chelminski et al. (2019).

The effects of sounds on marine mammals ranges from hearing injury to behavioral changes to masking of their hearing bands:

- American regulations provide the best available guidance for possible hearing injury to marine mammals in NMFS (2018). These regulations employ a dual criterion for prediction of hearing injury: the peak sound pressure level (PK), and the auditory frequency weighted daily sound exposure level (SEL; total daily sound energy) (Table 1).
- Behavioral disturbances are assessed using several approaches. The default approach compares the per-pulse sound pressure levels to an unweighted threshold of 160 dB re 1Pa^2. A more refined approach is a graded probability of response for impulsive sounds using a frequency-weighted sound exposure level (SPL) metric proposed by Wood et al. (2012) (Table 2). They also designated behavioral response categories for sensitive species (including harbor porpoises and beaked whales) and for migrating mysticetes. Their metric is also the per-pulse SPL but weighted by the older 'M-Weighting' proposed by Southall et al. (2007) (see Appendix B.4).
- Masking of biologically relevant sounds is perhaps the most pervasive effect of human sounds in the ocean (Erbe et al. 2016), however there are no regulations for acceptable thresholds of masking.

For clarity, this report refers to the frequency weighting defined in NMFS (2018) as the auditory frequency weighting functions, and the older weightings recommended by Southall et al. (2007) as M-weightings.

Table 1. Peak sound pressure level (PK; dB re 1 µPa), and sound exposure level (SEL; dB re 1 µPa^2 s) thresholds for, auditory injury (PTS onset), and TTS onset for marine mammals for impulsive sounds, as recommended by NMFS (2018). Low-frequency (LF) cetaceans are baleen or mysticete whales. Mid-frequency (MF) cetaceans are dolphins and sperm, killer, pilot, and beaked whales. High-frequency (HF) cetaceans are porpoise, high-frequency dolphins, and dwarf and pygmy sperm whales. Otariid pinnipeds are eared seals (fur seals and sea lions), and for purpose of the regulations they include otters and polar bears. Phocid seals are earless 'true' seals, and for purposes of the regulations include walrus.

Hearing group	Auditory injury (PTS)		TTS	
	Weighted SEL_{24h}	PK	Weighted SEL_{24h}	PK
LF cetaceans	183	219	168	213
MF cetaceans	185	230	170	224
HF cetaceans	155	202	140	196
Otariid pinnipeds in water	203	232	188	226
Phocid pinnipeds in water	185	218	170	212

Table 2. Wood et al. (2012) acoustic sound pressure level (SPL) thresholds used to evaluate potential behavioral impacts to marine mammals. Probabilities are not additive.

Marine mammal group	Species in Gulf of Mexico	Southall et al. (2007) frequency weighted probabilistic response (L_p; dB re 1 µPa)			
		>120	>140	>160	>180
Sensitive odontocetes	Dwarf / Pygmy sperm whales, beaked whales	50 %	90 %	–	–
Migrating mysticete whales	Rice's whale	10 %	50 %	90 %	–
All other species		–	10 %	50 %	90 %

2. Methods

2.1. Measured Sound Sources

The main sound source of interest for this verification was a 28000 in^3 tuned pulse source (TPS). Single TPS and dual TPS configurations were evaluated at 1000 psi air pressure. When operating dual TPS configurations, the units were separated by 20 m. For comparison, a 5000 in^3 standard seismic array (Figure 3) was also employed and the source vessel, the *Sanco Sword*, ran a stealth line without the seismic sources active. All sources were deployed at an 8 m depth. All sources were fired at a 1 pulse per minute rate.

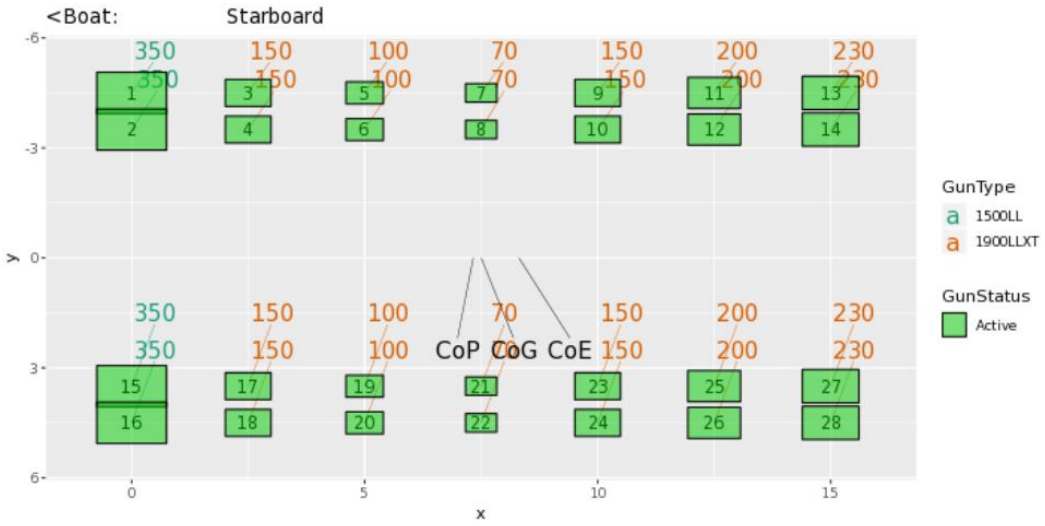

Figure 3. Configuration of the 5000 in^3 standard seismic array used for comparison to the TPS.

The active times (UTC) for each of the sources were as follows:

1. Single TPS: 2023-09-02 18:17 to 2023-09-03 05:53; CPA time: ~2023-09-03 02:01
2. Dual TPS: 2023-09-03 11:17 to 2023-09-03 23:57; CPA time: ~2023-09-03 19:56
3. 5000 in^3 airgun array: 2023-09-04 19:02 to 2023-09-05 06:04; CPA time: ~2023-09-05 02:27

For each source, the *Sanco Sword* conducted a pass starting at ~18000 m and transiting out to 23000 m past the receivers, and then conducted a series of close passes at various distances (Figure 4). The CPA times provided above are for station 5145. In addition to the passes with the pulse sources enabled, the vessel also performed a ‘stealth pass’ at 2023-09-04 05:00 without sources enabled along the same track as the long-range passes.

At the ends of the long-range pass, the bottom depth was ~200 m at the northern extent and ~900 m at the southern extent (Figure 5).

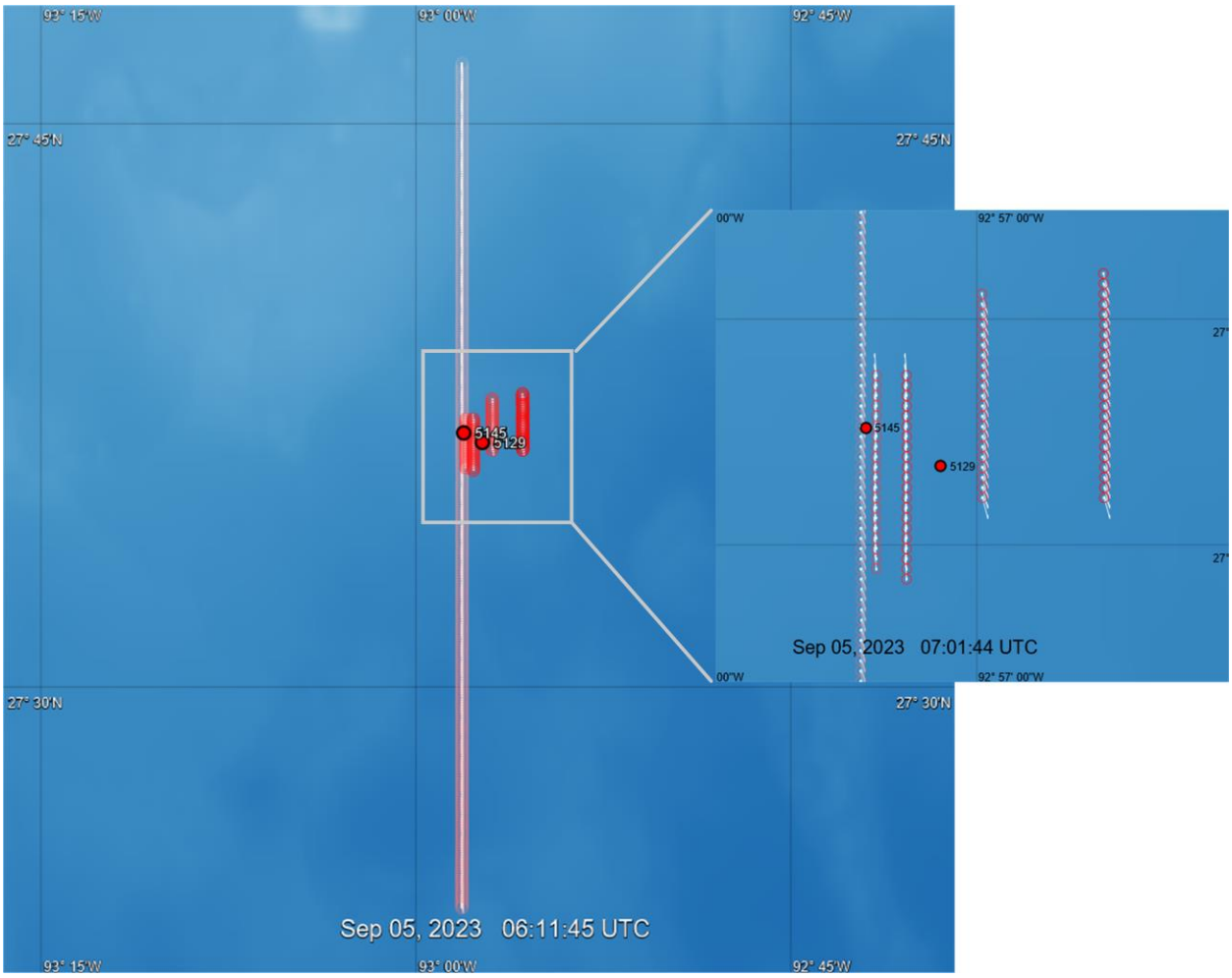

Figure 4. Track lines of the *Sanco Sword* during the airgun array exposures. The vessel track is shown as a white line underneath red circles at each of the points an airgun pulse occurred. The older pulses fade from red-pink-white. The track pattern features a main track line from 17500 m north to 20000 m south of the recorders with a CPA distance of 80 m, plus a broadside 'walk-away' pattern at 170, 670, 1920, and 3920 m from station 5145.

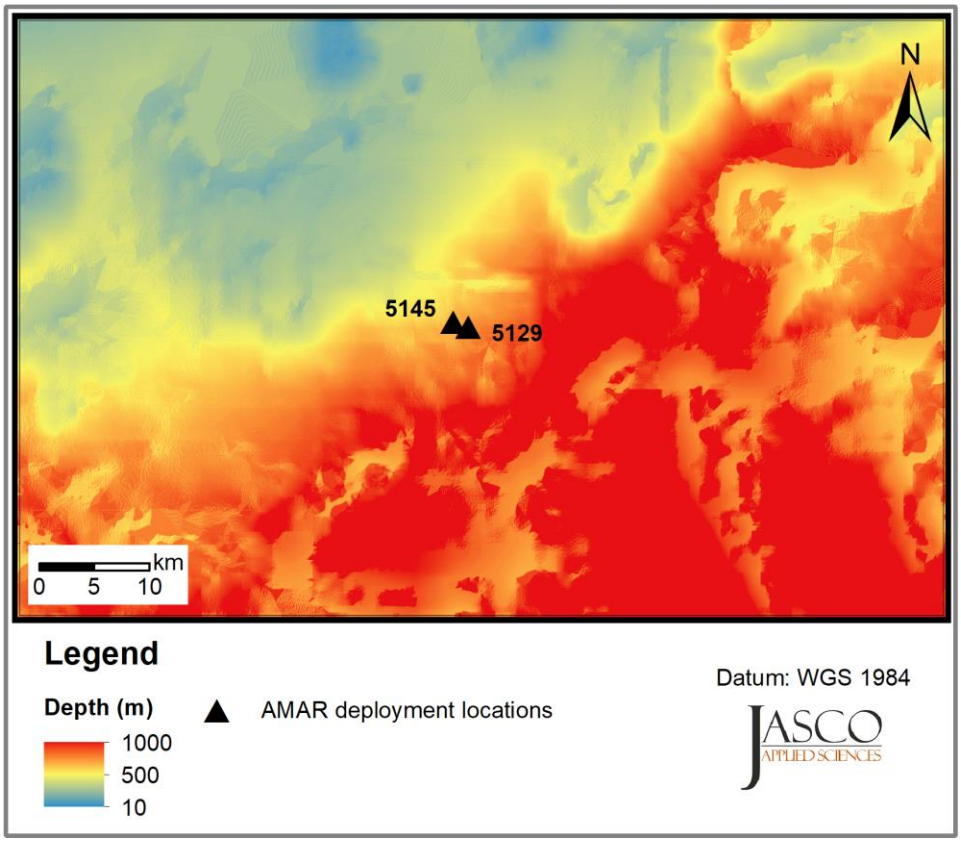

Figure 5. Bathymetry of the project area.

2.2. Acoustic Data Acquisition

2.2.1. Underwater Acoustic Recorders

Underwater sound was recorded with two Autonomous Multichannel Acoustic Recorders Generation 4 (AMAR G4, JASCO; Figure 6) in anodized aluminum housings. The AMARs recorded continuously over the 7-day recording period using internal 48-cell battery packs. Each AMAR was fitted with two M36 omnidirectional hydrophones (GeoSpectrum Technologies Inc., one with −165 ± 3 dB re 1 V/µPa sensitivity and the other with −200 ± 3 dB re 1 V/µPa sensitivity). The AMAR hydrophones were protected by a hydrophone cage and covered with an open-cell foam shroud to minimize non-acoustic noise caused by water flowing over the hydrophone transducer; this noise is often referred to as 'flow noise'. The AMARs recorded continuously at 128,000 samples per second for a recording bandwidth of 10 Hz to 64 kHz. The recording channel had 24-bit resolution with a spectral noise floor of 32 dB re 1 $\mu Pa^2/Hz$ and a nominal ceiling of 165 dB re 1 µPa for the hydrophone with a −165 dbV/µPa sensitivity level, and 57 dB re 1 $\mu Pa^2/Hz$ and a nominal ceiling of 200 dB re 1 µPa for the hydrophone with a −200 dbV/µPa sensitivity level. Acoustic data were stored on 2 TB of internal solid-state flash memory. Each AMAR was calibrated before deployment according to the procedure described in Appendix A.1 such that absolute sound pressure levels could be generated.



Figure 6. JASCO AMAR G4 in anodized aluminum housing (depth rated to 2500 m).

2.2.2. Deployment Locations

The AMARs were deployed in the operational area (Figure 7) between 1–7 Sep 2023. Figure 7 shows monitoring station locations, and Table 3 lists the location details. The AMARs were deployed from the *Marianne G* (Figure 8). The AMARs recorded as planned from deployment until retrieval.

Table 3. Description of measurement locations. Bathymetry of the area is shown in Figure 5.

Station ID	AMAR serial number	Water depth (m)	Lat (d°mm.mmm')	Long (d°mm.mmm')	Deployment	Retrieval	Duration (days)
5145	896	430	27° 36.78' N	92° 58.11' W	1 Sep 2023	7 Sep 2023	7
5129	890	455	27° 36.533' N	92° 57.365' W	1 Sep 2023	7 Sep 2023	7

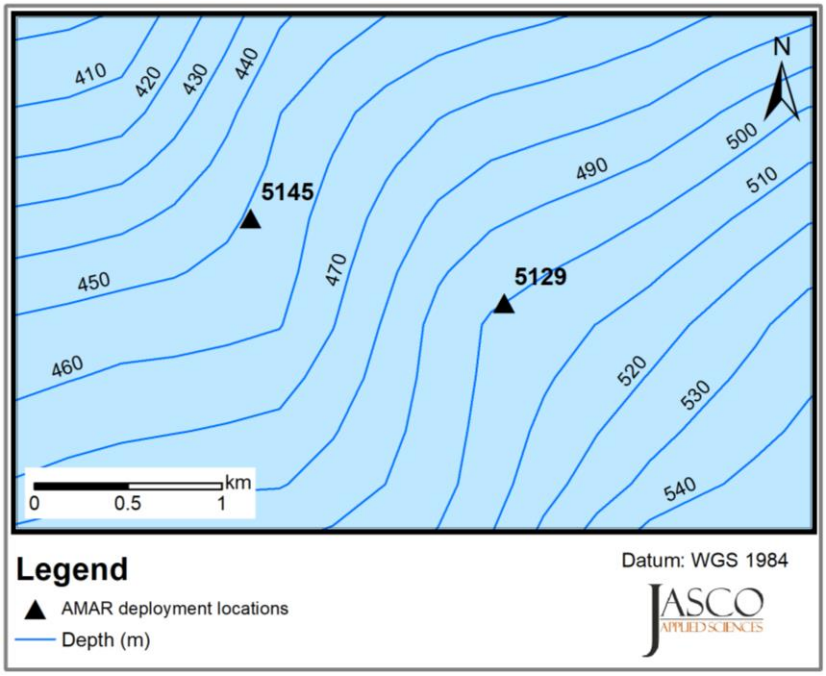

Figure 7. Deployment location of each AMAR showing depth contours.



Figure 8. Vessel *Marianne G* was used for deployment and retrieval operations.

2.2.3. Mooring Design

A 350 m long-line mooring (Figure 9) was used for the measurements, with the goal of positioning the hydrophones at ~100 m below the sea surface. A vectran rope was coated with ‘shakedown’ anti-strum coating to reduce strumming in the mooring. Two floats were used to keep the mooring tight and as buoyant as possible, again to reduce movement and strum in the mooring. Note that long-line moorings such as this move in currents despite the precautions taken. Modeling performed by JASCO suggests that the radius the hydrophone would rotate through (watch circle) would likely have been at most 75 m in radius, with up to 10 m of knockdown (Figure 10). Uncertainty in the hydrophone position affects estimates of the distance between the source and hydrophones for analysis of the received levels versus range. Since the hydrophones were 100 m below the source, the watch circle and knockdown added at most 30 m uncertainty in the slant range estimates used here. This would have a limited effect on the measured levels.

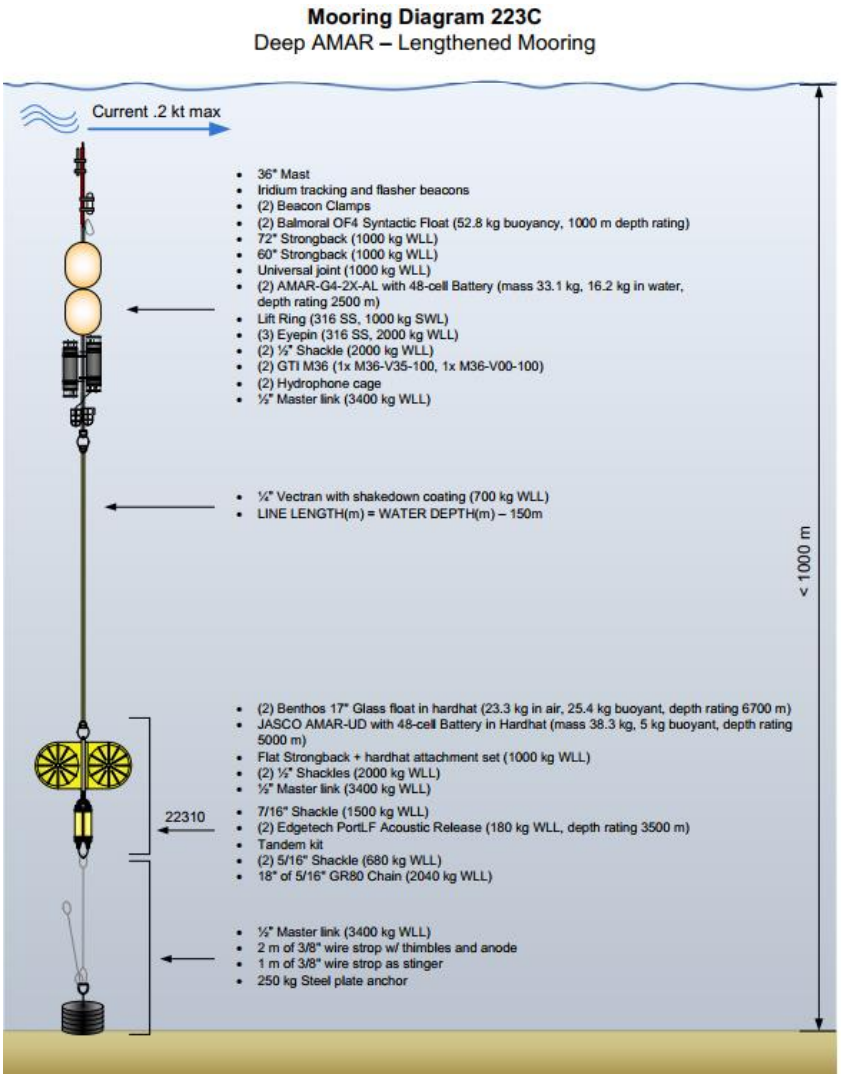

Figure 9. Mooring design employed for the TGS measurements.

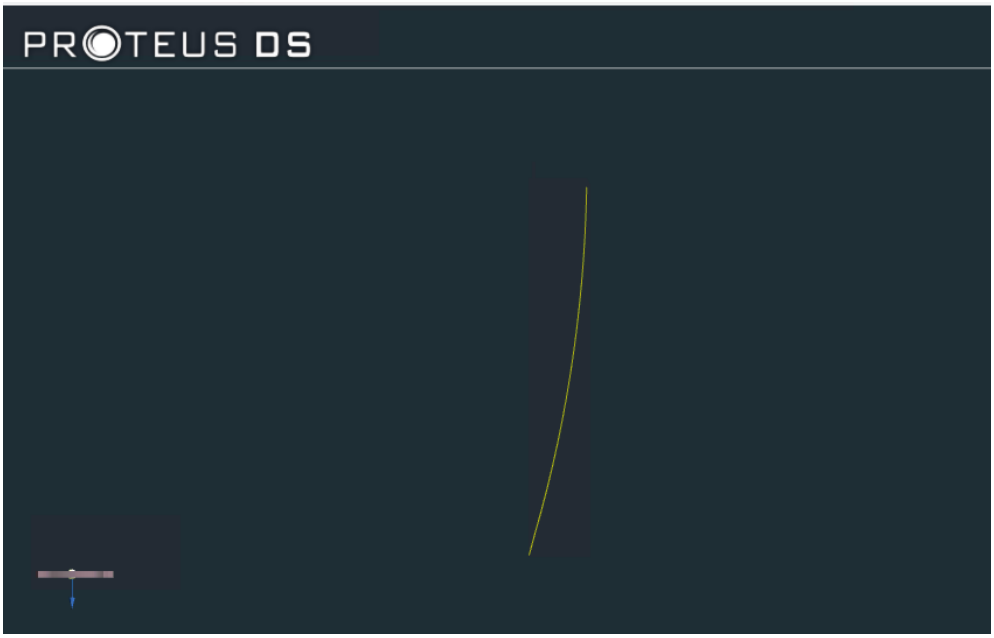

Figure 10. Model of the long mooring assuming 0.6 m/s of currents (a conservatively high value).

2.2.4. Acoustic Data Analysis

During the 7-day recording period, a combined 750 GB of acoustic data were collected at 128 kHz sample rate. The data were analyzed using a specialized computing platform capable of processing acoustic data hundreds of times faster than real-time. The system performed automated analysis to determine background or ambient sound characteristics, sounds from vessels and the seismic survey activities as well as sounds from marine mammals present in the vicinity of the recorders. The use of dual hydrophones (high and low sensitivity) allowed every pulse to be accurately quantified, with no data unusable due to either clipping (too loud) or being below background sound levels.

2.2.4.1. High Pass Filtering

The first stage in the analysis was to high-pass filter (HPF) the recorded data to remove frequencies below 10 Hz, which were affected by flow and movement noise. A linear phase finite impulse response (FIR) filter was employed as the HPF. Removing the energy below 10 Hz did not affect the assessment of the relative exposure of marine mammals to the different sources since those frequencies are heavily attenuated by the auditory frequency response functions (see Appendix B.4).

2.2.4.2. Pulse Detection and Analysis

In the first step of analysis, the digital recordings were converted to units of micropascals pressure (µPa) by applying the hydrophone sensitivity, the analog circuit frequency response, and the digital conversion gain of the AMAR. Next an automated detection algorithm identified the occurrence of the pulses and their start and end times by:

1. Bandpass filtering the 10 Hz HPF data to remove sound below 120 Hz and above 400 Hz. This provided the maximum signal-to-noise ratio of the recorded TPS pulses in the presence of vessel sound and flow noise on the hydrophones. A linear phase FIR was employed as the band-pass filter.
2. Squaring and summing the filtered time series every 50 ms to obtain a new energy time series, $X(t)$.
3. Evaluating the Teager-Kaiser energy (TKE) operator:

$$TKE = \frac{X^2(t)}{X(t+1)X(t-1)}$$

4. Comparing the TKE output to a detection threshold of 50; values above the threshold are identified as pulses for further processing.
5. For each pulse (for further information on metrics see Appendix B):
    a. Extracting the time span starting at 0.25 seconds before the start of the detection to 0.75 seconds after the start of detection *from the original time series* (HPF at 10 Hz).
    b. Squaring and summing the time series data to obtain an estimate of the total energy in the pulse.
    c. Starting at the beginning of the time series, squaring and summing the data until the energy is 5 % of the total found at Step (b). This marks the beginning of the pulse. Continue summing the time series until 95 % of the energy has been accumulated, which marks the end of the pulse. The time between the 5 and 95 % values is referred to as the 90 % duration of the pulse.
    d. Computing and saving the peak sound pressure level, sound pressure level, and sound exposure level of the pulse using the 90 % duration data.

e. Performing a fast-Fourier-transform (FFT) on the 90 % duration data to obtain the spectrum of the pulse, which was then saved as the per-pulse SEL in decidecade bands.

f. The loudness or magnitude of each recorded pulse was quantified by computing the peak pressure level (PK), 90 % duration SPL, and SEL of the pulse (defined in Appendix B.2).

For each airgun pulse recorded, the slant range to the source was computed from the GPS coordinates of the AMAR deployments and P1/11 files documenting the location of each TPS or airgun pulse. The location of the sources was taken as the center of the arrays or the location of the single TPS air nozzle.

Marine mammal frequency-weighted SEL were computed for each of the detected pulses for LF, MF, and HF cetaceans, respectively (see Appendix B.4). The frequency-weighted SEL from all received pulses were summed on a linear scale to yield the cumulative SEL.

2.2.4.3. Marine Mammal Detection

A combination of automated detector-classifiers (referred to as automated detectors) and manual review by experienced analysts were used to determine the presence of sounds produced by marine mammals in the acoustic data. First, a suite of automated detectors was applied to the full data set (see Appendices C.1 and C.2). Second, subsets (~2.8 %) of acoustic data were selected for manual analysis of marine mammal acoustic occurrence. Each subset was selected based on automated detector results via our Automatic Data Selection for Validation (ADSV) algorithm (Kowarski et al. 2021) (see Appendix C.3). Third, manual analysis results were compared to automated detector results to determine automated detector performance (see Appendix C.4). Finally, hourly marine mammal occurrence plots that incorporated both manual and automated detections were created and automated detector performance metrics were provided (see Section 3.6) to give a reliable representation of marine mammal presence in the acoustic data. These marine mammal analysis steps are summarized here and described in detail in Appendix C. Where automated detector results were unreliable or did not add additional information to species occurrence, only the validated results from manual analysis are presented.

2.2.4.3.1. Automated Click Detection

Odontocete clicks are high-frequency impulses ranging from 1 to over 150 kHz (Au et al. 1999, Møhl et al. 2000). An automated click detector was applied to the high-frequency data (audio bandwidth up to 256 kHz) to identify clicks from sperm whales, beaked whales, porpoises, and delphinids. This automated detector is based on zero-crossings in the acoustic time series. Zero-crossings are the rapid oscillations of a click's pressure waveform above and below the signal's normal level (e.g., see Figure C-1). Zero-crossing-based features of automatically detected events are then compared to templates of known clicks for classification (see Appendix C.1 for details).

2.2.4.3.2. Automated Tonal Signal Detection

Tonal signals are narrowband, often frequency-modulated, signals produced by many species across a range of taxa (e.g., baleen whale moans, delphinids whistles). They range predominantly from 15 Hz and 4 kHz (Berchok et al. 2006, Risch et al. 2007), thus automated detectors for these species were applied to the low-frequency data (audio bandwidth up to 16 kHz). In contrast, the automated detector for small dolphin tonal acoustic signals was applied to the high-frequency data, as these whistles can reach 20 kHz (Steiner 1981). The automated tonal signal detector identified continuous contours of elevated energy and classified them against a library of marine mammal signals (see Appendix C.2 for details).

2.2.4.3.3. Automated Detector Validation

JASCO's suite of automated detectors are developed, trained, and tested to be as reliable and broadly applicable as possible. However, the performance of marine mammal automated detectors varies across acoustic environments (e.g., Hodge et al. 2015, Širović et al. 2015, Erbs et al. 2017, Delarue et al. 2018). Therefore, automated detector results must always be supplemented by some level of manual review to evaluate automated detector performance. Here, a subset of acoustic files was manually analyzed for the presence/absence of marine mammal acoustic signals via a spectrogram review in JASCO's PAMlab software. A subset (2.8 %) of acoustic data was selected via ADSV for manual review (see Appendix C.3).

To determine the performance of the automated detectors per acoustic file, the automated and manual results (excluding files where an analyst indicated uncertainty in species occurrence) were fed into an algorithm that calculates precision (*P*), recall (*R*), and Matthew's Correlation Coefficient (*MCC*) (see Appendix C.4 for formulas). *P* represents the proportion of files with detections that are true positives. A *P* value of 0.90 means that 90 % of the files with automated detections truly contain the targeted signal, but it does not indicate whether all files containing acoustic signals from the species were identified. *R* represents the proportion of files containing the signals of interest that were identified by the automated detector. An *R* value of 0.90 means that 90 % of files known to contain a target signal had automated detections, but it says nothing about how many files with automated detections were incorrect. An MCC is a combined measure of *P* and *R*, where an MCC of 1.00 indicates perfect performance: all known events were correctly automatically detected. The algorithm determines a per file automated detector threshold (the number of automated detections per file at and above which automated detections were considered valid) that maximizes the MCC.

For many species, more than one automated detector targeted their vocalizations. In these instances, the performance of all automated detectors was evaluated, and the highest performing detector (or combination of detectors) used to represent species/vocalization-type occurrence in Section 3.6. Only automated detections associated with a *P* greater than or equal to 0.75 were considered. When $P < 0.75$, only the validated results were used to describe the acoustic occurrence of a species.

The occurrence of each species (both validated and automated, or validated only where appropriate) was plotted using JASCO's Ark software as time series showing presence/absence by hour over each day of the recording period and daily count of detection hours, where necessary. Automated detector performance metrics associated with results (included in Section 3.6) should be considered when interpreting results.

2.2.4.4. Available Listening Range

To provide a relative estimate of masking by the sound sources, the available listening range (ALR) was computed. ALR estimates how the percentage of the maximum possible listening range for marine life changes as a function of time. It is similar to the concept of listening space reduction (Pine et al. 2020) that estimates how much of an animal's listening range is lost due to a masking noise source. ALR is computed using the sound levels in specific critical hearing bands (see Equation 1). In Equation 1, NL_2 is the sound pressure level at the time analyzed, NL_1 is the lowest typical sound pressure level, and N is the geometric spreading coefficient for the acoustic propagation environment. If an animal's threshold of hearing is higher than NL_1, NL_1 is replaced with the hearing threshold. The sound pressure levels are computed for decidecade bands that are representative of the important listening frequencies for animals of interest.

$$\mathrm{ALR} = 100 * (10^{\frac{NL_2 - NL_1}{N}}) \quad (1)$$

ALR was computed to assess how the listening range changed in the presence of the TPS and airgun pulses. Since the integration time for mammalian hearing is ~0.1 seconds, this duration was chosen as the analysis window. The critical bandwidth for marine mammals is approximately 1 decidecade wide, which set the analysis bandwidths considered. The analysis was performed to assess how the sources could mask the downsweeping calls from Rice's whales (80 Hz decidecade) and the whistles of dolphins (10000 Hz decidecade). The value of NL_1 was chosen to be the 10th percentile of sound pressure level in each decidecade band, that is the SPL that exceeded the lowest 10% of the 0.1 sec samples over the duration of the recording program. The ALR were computed for the 20 seconds following each pulse for the Rice's whales, and for the 10 seconds following each pulse for the dolphin whistles. The analysis was performed using the data from Station 5145 for the main overpass events (see Figure 4). The geometric spreading coefficients were estimated for each of passes independently.

3. Results

3.1. Total Sound Levels

Figure 11 summarizes the recording from station 5145. The data in Figure 11 does not include the 10 Hz high pass filter applied to show why it was employed. The key sound events from the trials are annotated in the spectrogram.

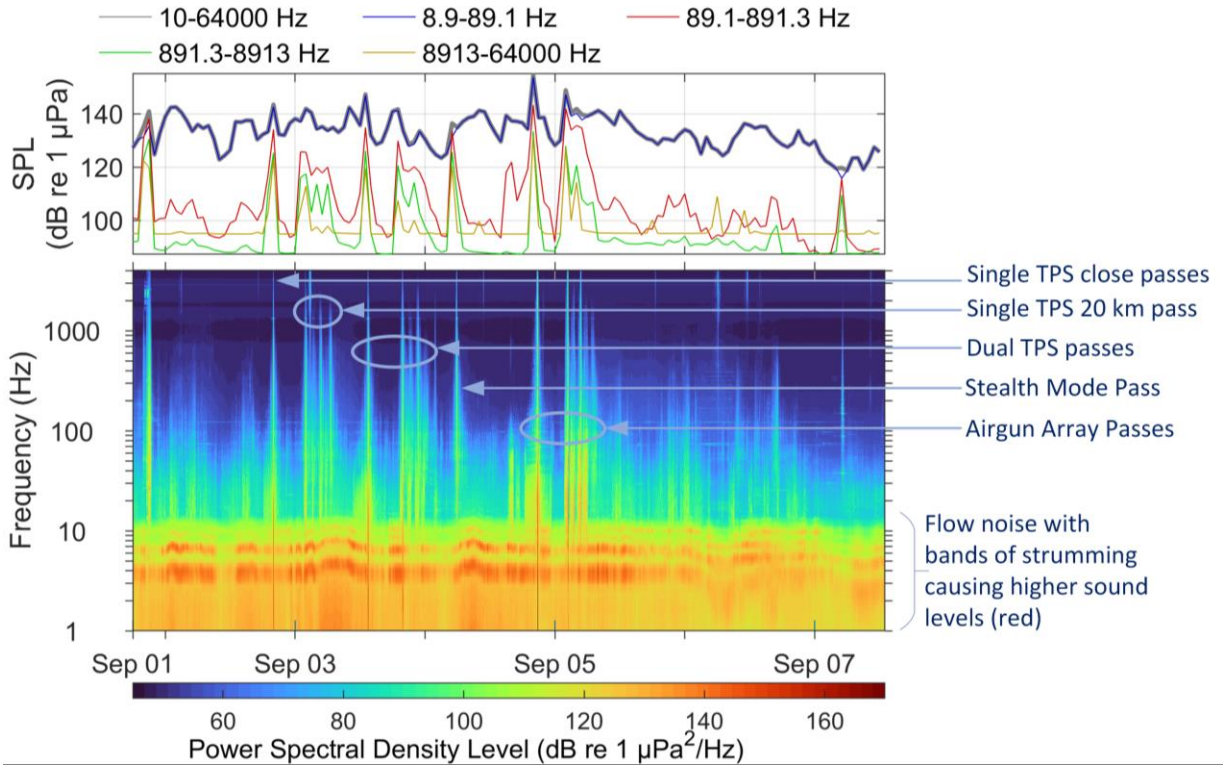

Figure 11. Total sound level summary from station 5145: (Top) Hourly in-band sound pressure level and (bottom) long term spectrogram average (LTSA) of received sound for the duration of the deployment. The LTSA is annotated with the significant trial events. The spectrogram has been limited to a maximum frequency of 4 kHz to focus on the trial events.

3.2. Received Levels from the Pulsed Sources

The peak sound pressure levels from the TPS were ~10 dB lower than those from the seismic airgun array (Figures 12 and 13). Starting at ~5 km from the receiver, the peak sound pressure levels appear to have two sets of values that also differ by ~10 dB (Figure 13). These are related to the northern and southern directions, presumably due to substantially different propagation environments with the changes in water depth (see Figures 5 and 13).

The lower peak sound pressure levels from the TPS resulted in substantially reduced high-frequency content, which is clearly visible from the spectrogram in Figure 12. By applying the marine mammal auditory frequency weighting filters, the differences in the per-pulse sound exposure levels are ~10 dB for LF mammals, and 30 dB for the MF and HF mammals (Figure 15). The differences between the northern

(shallow) and southern (deep) data remain visible for the LF mammals; however, they are not present for the MF and HF mammals because the sound levels reach the system noise floor at ~ 2 km. The differences in peak sound pressure level and frequency content did not result in differences in pulse durations (Figure 16).

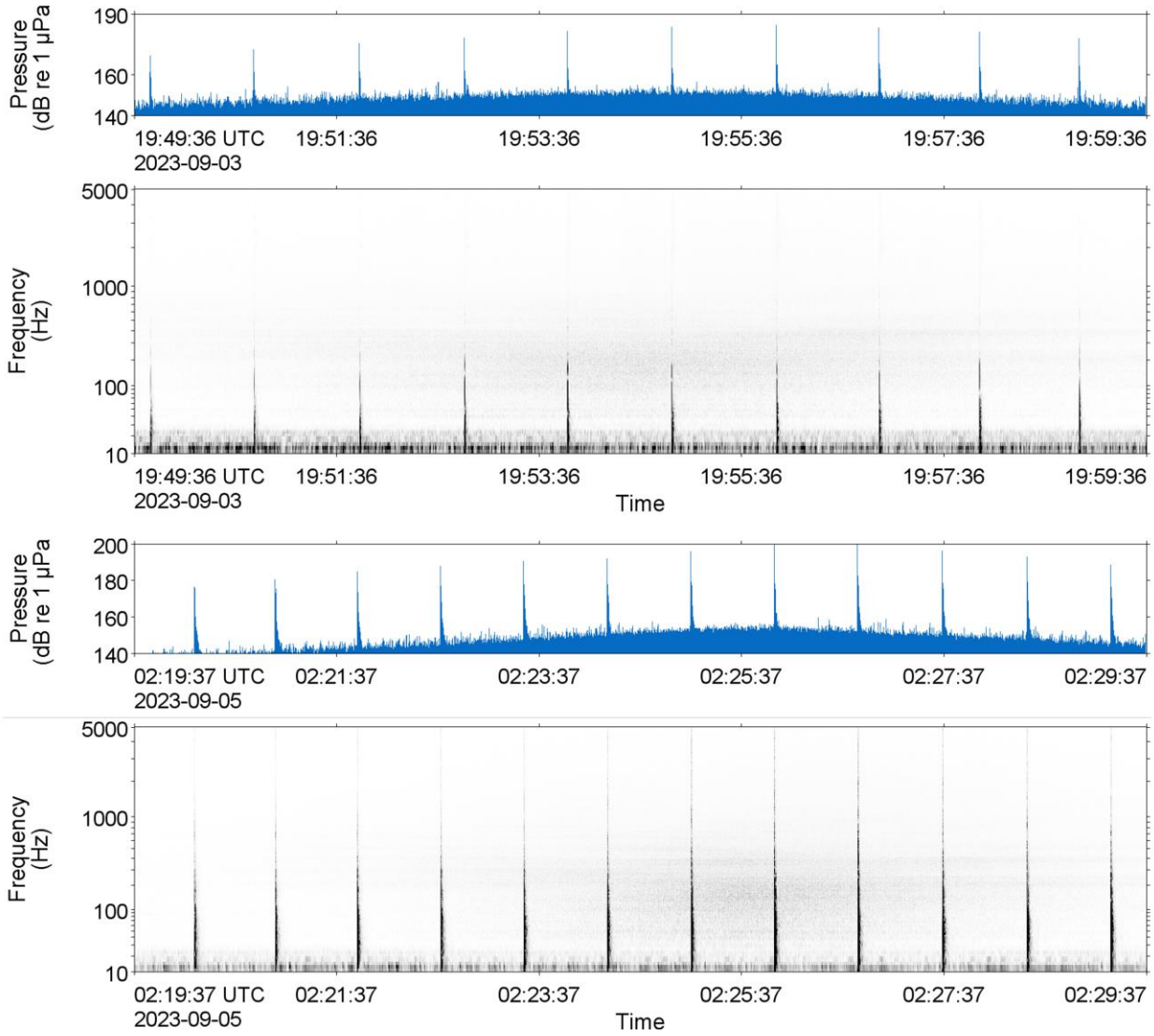

Figure 12. Comparison of the received levels from (top) the dual TPS pass versus (bottom) the airgun array pass, at the closest points of approach (CPA) to station 5145 (80 m). For each source, the top figure is the broadband (10–64000 Hz) received sound pressure level, and the bottom is the spectrogram (2 Hz resolution, 0.5 s of data used in the FFT with 0.25 s advance). Note the difference in scale for the time series. The spectrograms are plotted with a fixed dynamic range for the power spectral density of 90 to 140 dB re 1 µPa²/Hz.

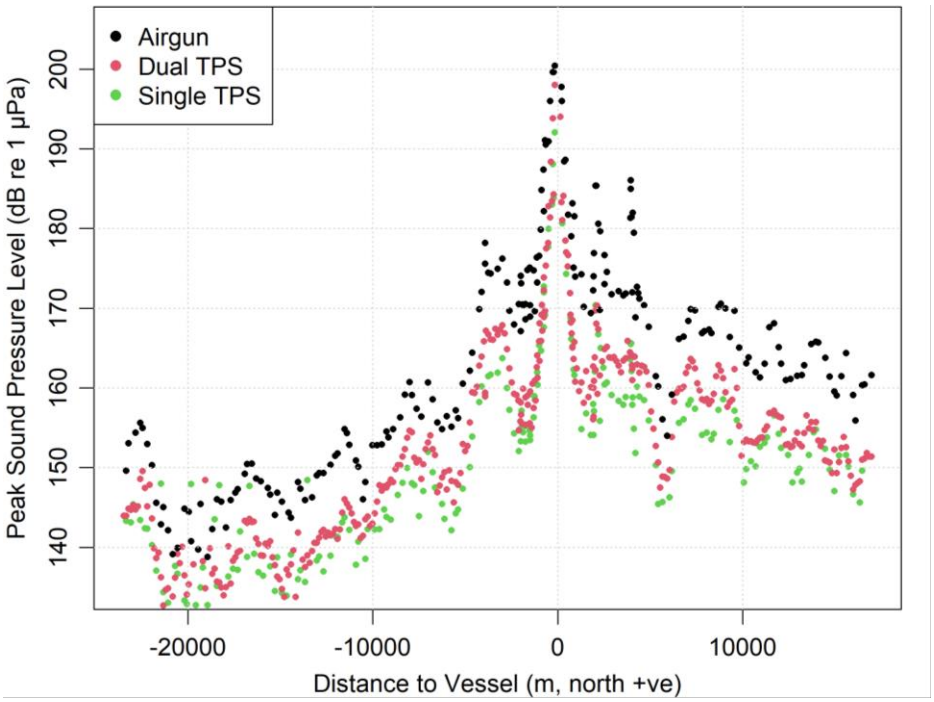

Figure 13. Peak sound pressure level (PK) as a function of distance to the source using data recorder 5145. The levels are ~10 dB different to the south in deep water compared to the north with its shallow water depths. Positive and negative values on the x-axis show distances to the north and south of the recorder, respectively.

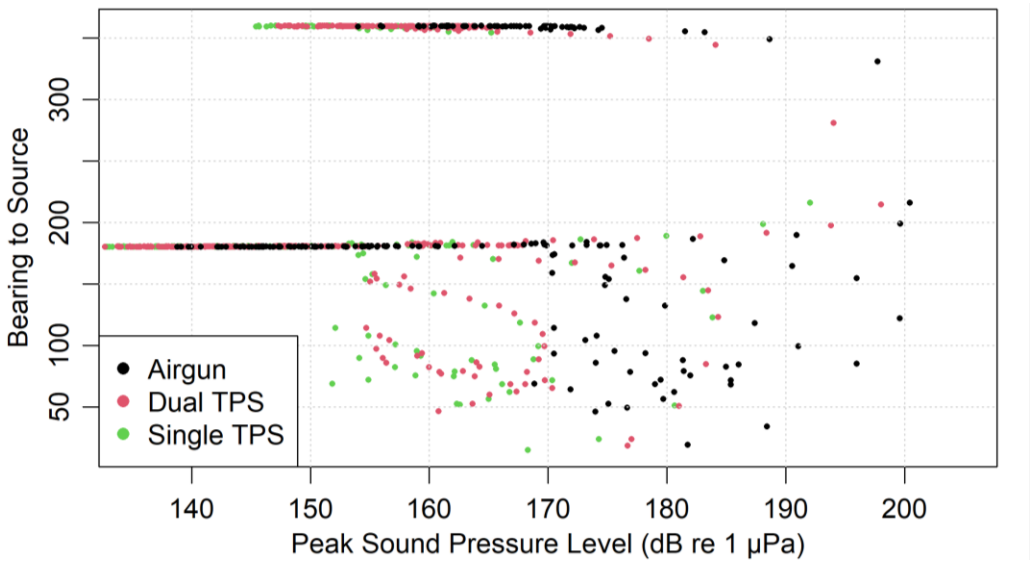

Figure 14. Peak sound pressure levels (PK) as a function of direction to the vessel from Station 5145.

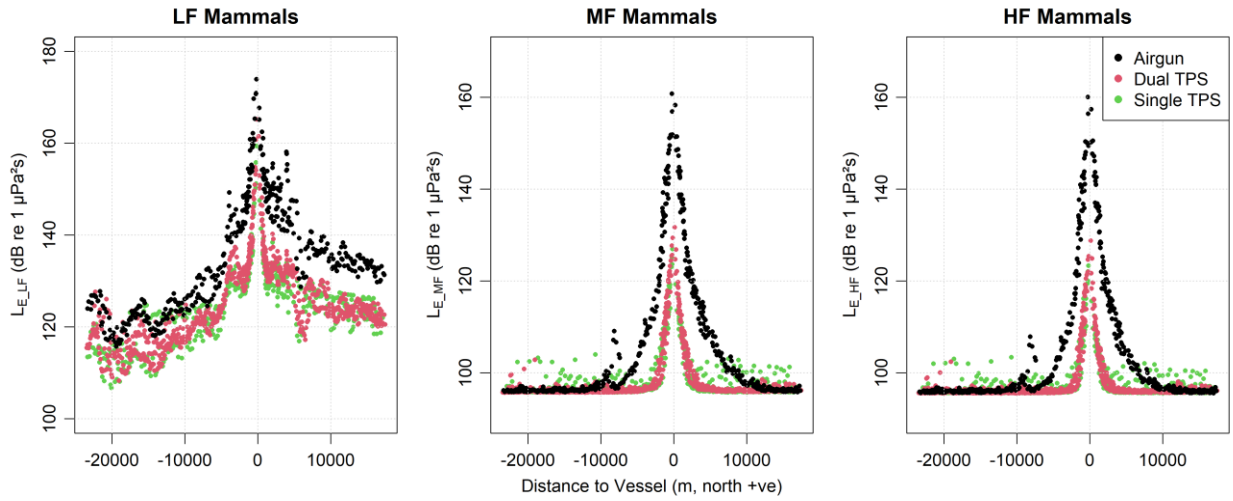

Figure 15. Per pulse auditory frequency weighted sound exposure levels for all detected pulses as a function of absolute value of the distance to the source type (color). Note that the low-frequency (LF) mammal vertical scale is 110–180 dB compared to 90–170 dB for the mid-frequency (MF) and high-frequency (HF) mammals. Positive and negative values on the x-axis show distances to the north and south of the recorder, respectively.

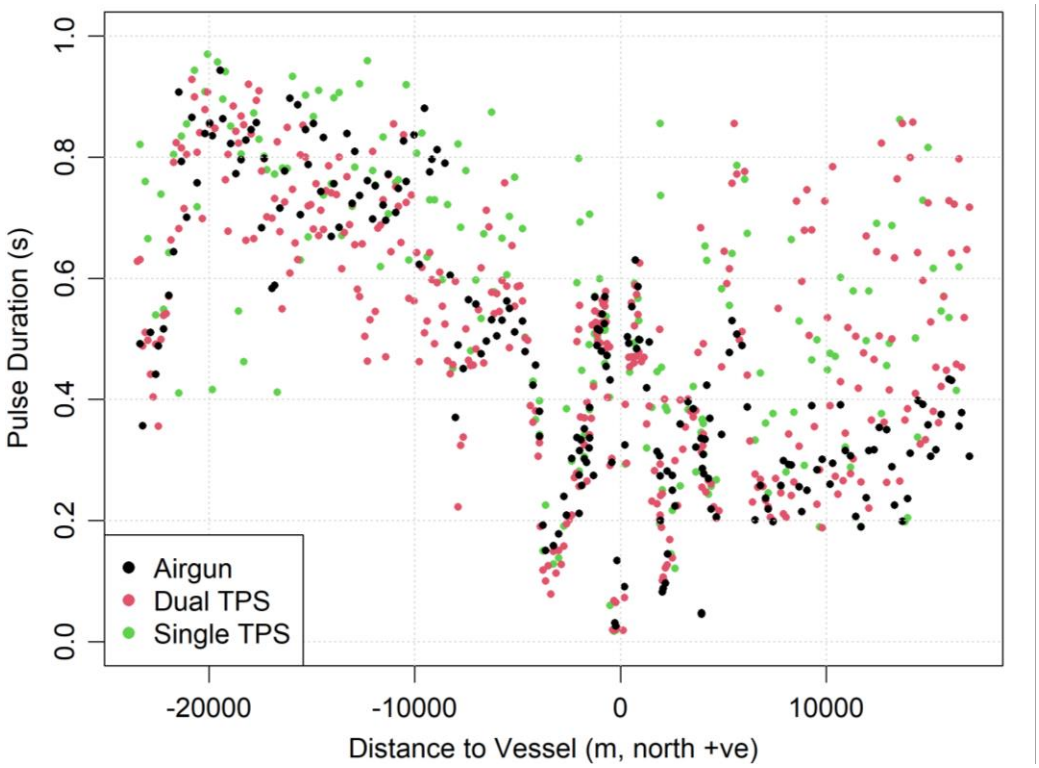

Figure 16. Pulse duration versus range by source type. Positive and negative values on the x-axis show distances to the north and south of the recorder, respectively.

3.3. Cumulative Sound Exposure Levels

The relative cumulative sound exposure levels from each of the sources are particularly relevant results as they directly relate to the thresholds for sound exposure in marine mammals (NMFS 2018, Southall et al. 2019). The single TPS SEL were 16–19 dB below those of the airgun array for LF mammals, and 31–35 dB below for HF and VHF mammals. The dual TPS had a slightly higher SEL, as expected. It was 10–14 dB lower than the airgun array for LF mammals and 28–29 dB lower for the MF and HF mammals (Figure 17). The airgun array exceeded the PTS threshold for HF mammals and TTS threshold for LF mammals at both locations (Figure 17). The TTS threshold was exceeded by the dual TPS configuration for LF mammals at station 5145 at the CPA distance of 80 m. The dual TPS configuration remained below the HF mammal TTS threshold even at this close distance.

The SEL was strongly linked to the CPA of the source to the receiver (Figures 4 and 17). The CPA distances were 7 times shorter at station 5145 compared to those at 5129, which resulted in levels 5–10 dB higher for the LF mammals and 3–7 dB for the MF and HF mammals. Note that the SEL also depends on the number of pulses emitted. If the pulse rate were increased to a more typical pulse every 20 seconds, the SEL would increase by $10\log_{10}(3)$, i.e., ~5 dB. This would push the single TPS configuration to the LF TTS threshold and the dual TPS configuration to the HF TTS thresholds with a CPA range of 80 m.

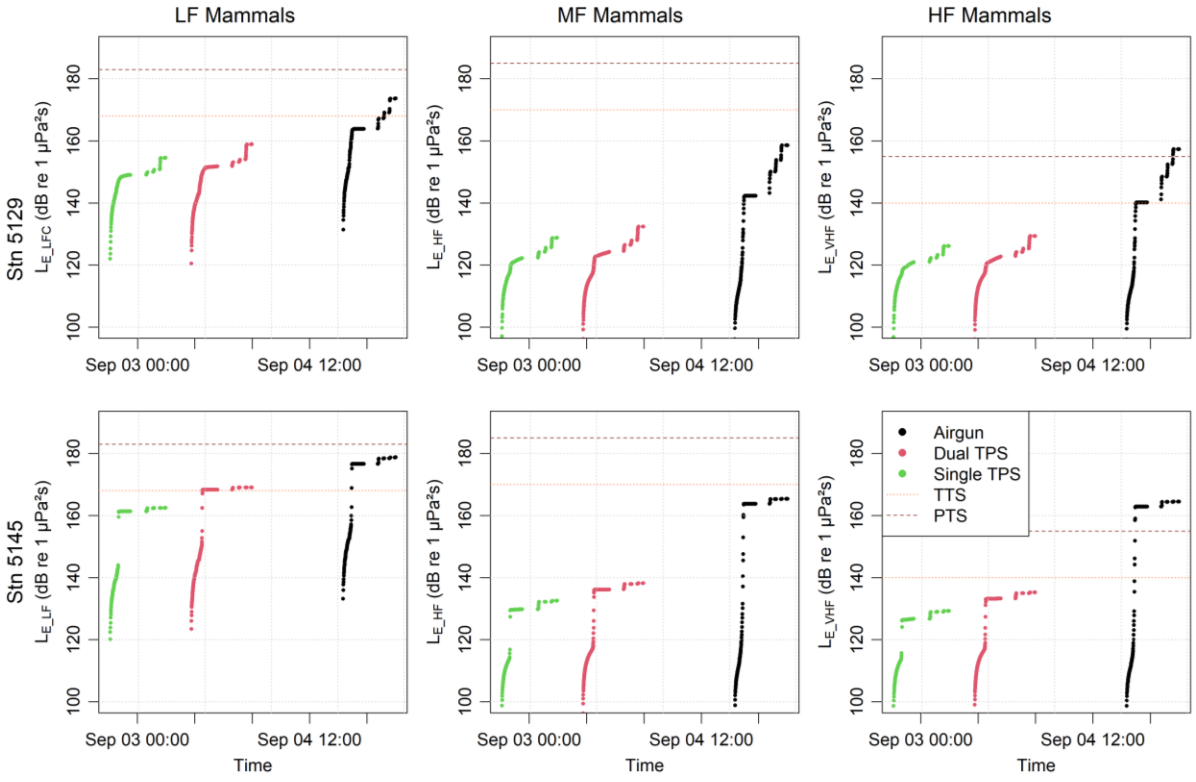

Figure 17. Cumulative marine mammal weighted sound exposure levels for each of the stations and source types. The NMFS 2018 thresholds for temporary and permanent threshold shifts are included as horizontal lines.

Table 4. Auditory frequency weighted cumulative sound exposure levels for each source and station.

Station	Source	CPA[1] distance (m)	$L_{E,w}$ (dB re 1 µPa²s)		
			LF mammals[2]	MF mammals[2]	HF mammals[2]
5129	Single TPS	560	154.6	126.1	126.1
	Dual TPS	560	158.9	129.3	129.3
	Airgun Array	550	173.7	157.3	157.3
5145	Single TPS	80	162.5	129.3	129.3
	Dual TPS	80	169.0	135.2	135.2
	Airgun Array	80	178.8	164.4	164.4

[1] Closest point of approach

[2] Low-frequency, mid-frequency, and high-frequency

3.4. Behavioral Disturbance

The per-pulse 90 % duration sound pressure levels were estimated by adding 10*log10(90 % duration) to the Southall et al. (2007) M-weighted per-pulse sound exposure levels from Station 5145 (Figure 18, Station 5129 was excluded due to higher noise levels at low frequencies that contaminated the analysis when using the Southall et al (2007) M-weightings). The SPLs show the clear differences between the northern (shallow) and southern (deeper) propagation conditions with greater differences between the airgun and the TPS in the shallower waters. The SPLs for each source were fit to equations of the form $SPL = A + B\log_{10} R$, where R is the distance to the vessel (100–15000 m), *A* is the effective source level, and *B* is the effective geometric spreading coefficient (see Table 5). This type of data fit is valid only for the conditions measured. The fits were much better in the deep waters than the shallow, likely due to the occurrence of several spikes at shorter ranges that corresponded to very short pulse durations (see Figures 15 and 18).

The fit equations are useful for predicting the distance at which the SPLs drop below the Wood et al. (2012) behavioral disturbance thresholds (Table 2) to obtain the distances at which marine mammals are likely to react to the sources (Table 6). The disturbance distances were limited to the 20 km to avoid extrapolating far beyond the distances measured.

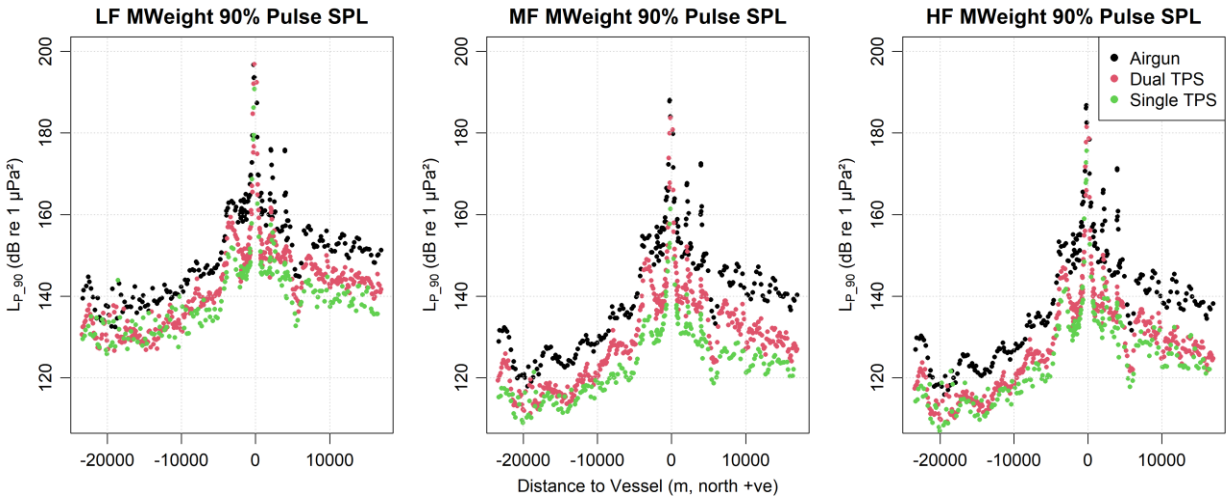

Figure 18. Received per-pulse M-Weighted sound pressure levels as a function of the source and distance from Station 5145 to the sources. Positive and negative values on the x-axis show distances to the north and south of the recorder, respectively.

Table 5. Linear model fit parameters for the per-pulse SPLs in Figure 18 (weighted by the Southall et al (2007) M-weighting), to the equation $SPL = A + B\log_{10} R$, where R is the distance to the vessel (100–15000 m), *A* is the effective source level, and *B* is the effective geometric spreading coefficient. Note that these values are only valid for the location and sources measured, as evidenced by the substantial differences between the shallow (north of recorder) and deep (south of recorder) parameters.

Southall et al (2007) M-Weighting Group	Water Depth	Effective Source Levels (dB re 1 µpa²)	Effective Geometric Spreading Coefficient	r2 (Coefficient of Determination)
Airgun				
LF	Shallow	206.5	-13.4	0.54
	Deep	246.5	-26.0	0.92
MF	Shallow	206.8	-15.8	0.56
	Deep	253.9	-30.9	0.94
HF	Shallow	206.9	-16.3	0.57
	Deep	253.7	-31.3	0.94
Single TPS				
LF	Shallow	180.0	-9.9	0.57
	Deep	220.5	-21.9	0.79
MF	Shallow	176.5	-12.0	0.57
	Deep	223.7	-26.3	0.86
HF	Shallow	175.3	-12.3	0.58
	Deep	222.5	-26.5	0.86
Dual TPS				
LF	Shallow	189.8	-11.3	0.58
	Deep	224.7	-22.3	0.78
MF	Shallow	188.8	-14.3	0.67
	Deep	224.0	-25.4	0.83
HF	Shallow	187.8	-14.6	0.68
	Deep	222.9	-25.7	0.84

Table 6. Distances (m) to the Wood et al (2012) SPL thresholds for behavioral disturbance for species or groups that could occur in the project area (see Table 2). SPLs are M-weighted (Southall et al 2007). Distances were computed by finding the distance at which the linear equations from Table 5 fall below the disturbance thresholds. The maximum distance computed was 20000 m to avoid extrapolating far beyond the maximum distances measured.

		Rice's Whale (LF)			Dwarf and Pygmy Sperm Whales (HF)		Beaked Whales (MF)		All Other Odontocetes (MF)		
Source	Water Depth	10% (120 dB)	50% (140 dB)	90% (160 dB)	50% (120 dB)	90% (140 dB)	50% (120 dB)	90% (140 dB)	10% (140 dB)	50% (160 dB)	90% (180 dB)
Airgun	Shallow	>20000	>20000	3030	>20000	2540	>20000	17130	17130	930	50
	Deep	>20000	12580	2140	18550	4270	>20000	4890	4890	1100	250
Single TPS	Shallow	>20000	10420	110	>20000	780	>20000	1080	1080	30	10
	Deep	>20000	4720	580	7420	1310	8830	1530	1530	270	50
Dual TPS	Shallow	>20000	>20000	430	>20000	1860	>20000	2540	2540	110	10
	Deep	>20000	6140	790	10130	1690	12280	2010	2010	330	60

3.5. Masking of Biologically Relevant Sounds

As described in Section 2.2.4.4, the potential for the sources to mask marine mammal vocalizations were assessed using the available listening range. The geometric spreading coefficient, N, employed for the ALR analysis was the average of the M-weighting dependent effective spreading coefficients computed from the behavioral disturbance analysis (Table 5). For the shallow water conditions, the LF, MF, and HF averages were 11.5, 14.0, and 14.4; for the deep water conditions the respective values were 23.4, 27.5 and 27.8. The listening range is limited by the sound in the environment in both cases rather than by the animal's hearing.

The computed ALR are shown in Figures 19 and 20. ALR estimates the percentage of the best-case listening range that the animals had available as the sources and vessel passed by Station 5145. For impulsive sources like the airguns or TPS, we expect a reverberant decay in the received levels as a function of time after the pulse. The reverberation levels should be higher when the sources are closer to the recording location. An example of this 'classic' impulsive masking occurred with the airgun for the dolphin whistles in the top row of Figure 23, and to a lesser extent in for the airgun's effects on the Rice's whale in Figure 19.

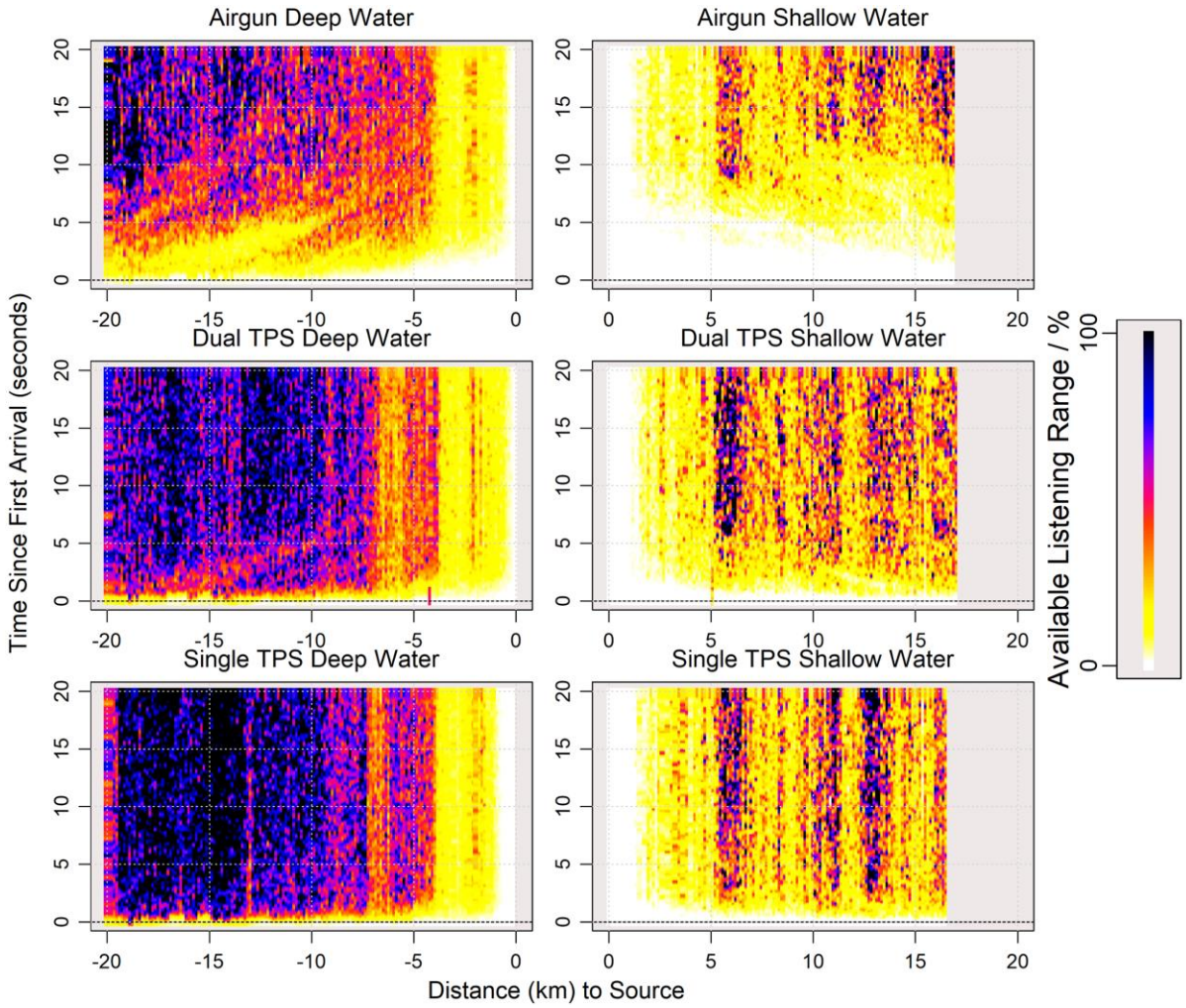

Figure 19. Available Listening Range (100 % is good) at Station 5145 for Rice's whale 80 Hz downsweeps. Negative distances are south of the recorder, positive distances to its north.

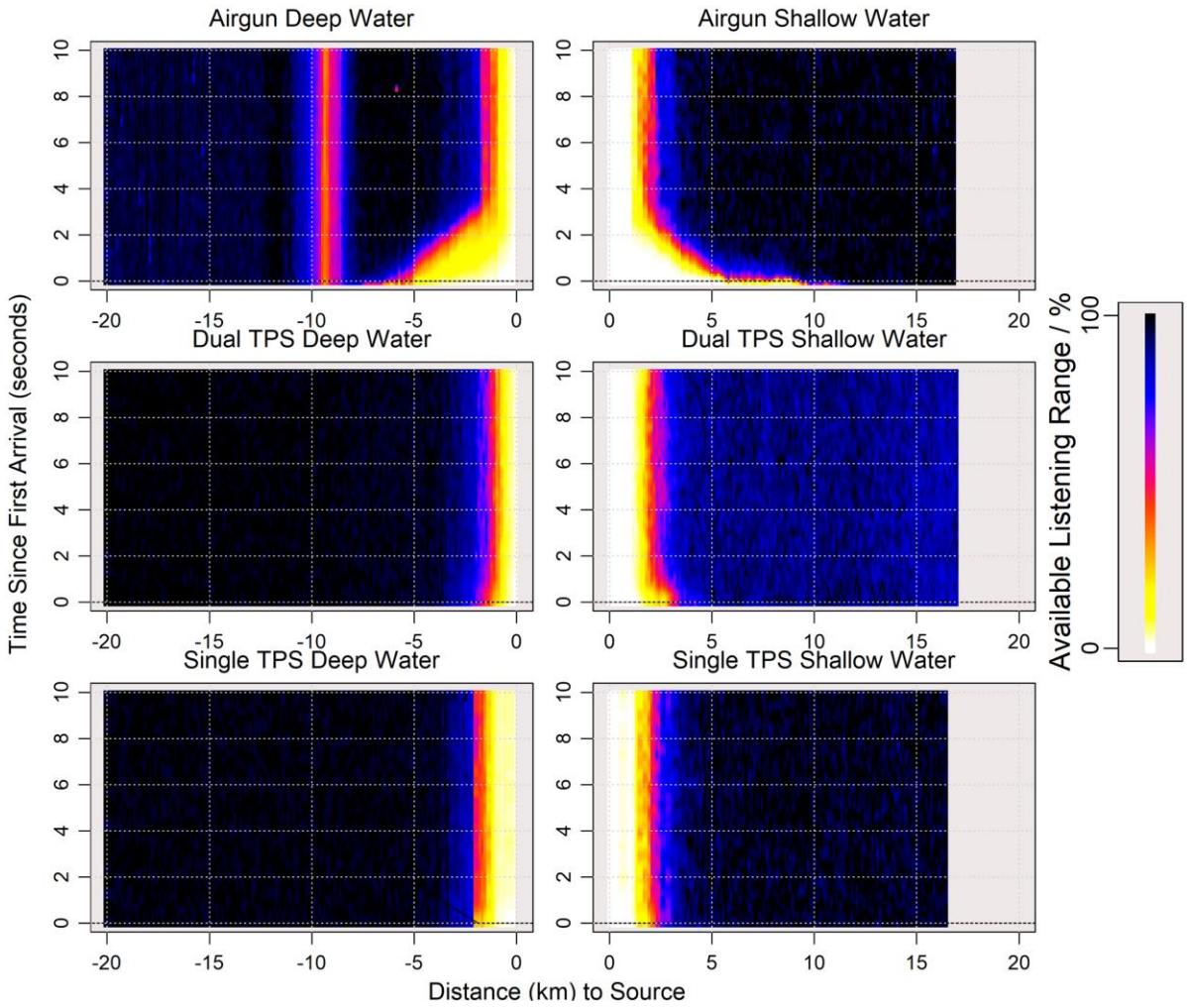

Figure 20. Available Listening Range (100 % is good) at Station 5145 for dolphin whistles at 10000 Hz. Negative distances are south of the recorder, positive distances to its north.

Table 7. Decidecade bands analyzed for the Available Listening Range. If the audiogram level is above the 10th percentile of the 0.1 second decidecade SPL across the full deployment duration, then the species was *hearing* limited rather than *noise* limited. Audiogram sensitivity was based on Finneran (2016).

Species or group	Decidecade band centre frequency (Hz)	10th percentile of measured 0.1 s decidecade SPL (dB re 1 µPa²)	Audiogram level (hearing sensitivity, dB re 1 µPa²)
Rice's Whale	80	91.8	68.1
Dolphin Whistles	10000	81.8	64.5

3.6. Marine Mammal Detections and Exposure

3.6.1. Detector Performance

The manual analysis of data revealed the presence of three types of signals: sperm whale clicks, (Section 3.6.2) and delphinid whistles and clicks (Section 3.6.3). The sperm whale click automated detector performed poorly on these data, presumably because of the high sound levels at frequencies overlapping with the signals. The dolphin whistle and click detectors performed well (Table 8), with similar performance metrics at both stations.

Table 8. Automated detector performance including the threshold implemented (minimum number of automated detections per file for species to be considered present) and the original and final detector precision (*P*), recall (*R*) and MCC score. The final automated detector performance values (Final) represent the performance after any timeframe and/or threshold restrictions have been applied. TP: true positive; FP: false positive; FN: false negative; TN: true negative.

Species/group (vocalization)	Station	Automated detector	Exclusion period	Per-file threshold	Final						
					P	*R*	*MCC*	*TP*	*FP*	*FN*	*TN*
Dolphin (whistle)	5129	WhistleHighLoud	None	4	1.00	0.29	0.45	10	0	24	55
	5145			4	1.00	0.36	0.53	10	0	18	68
Delphinid clicks	5129	KillerWhaleClickTrain	None	1	0.95	0.65	0.71	20	1	11	66
	5145			1	0.89	0.67	0.71	16	2	8	69

3.6.2. Sperm Whales

Sperm whale clicks (Figure 21) were detected manually at both stations. Detections occurred for up to 4 hours per day on every day of the recording period except for the last day (Figures 22 and 23).

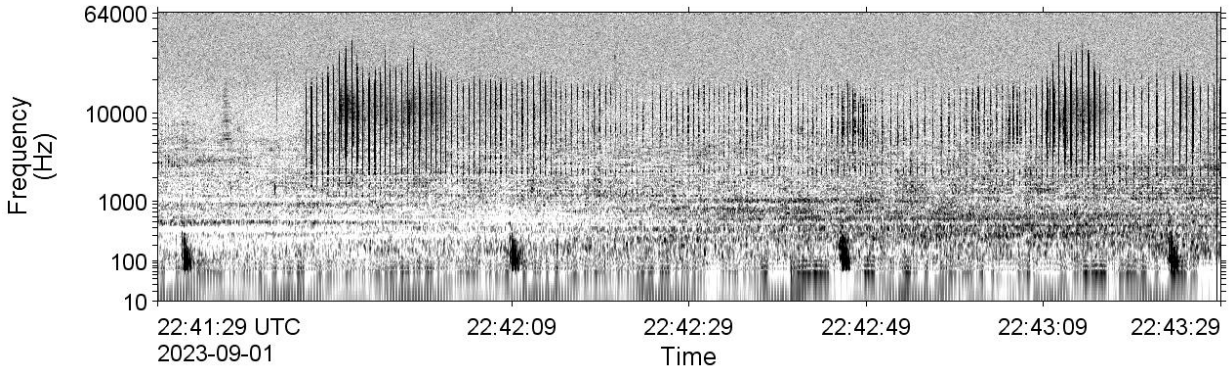

Figure 21. Sperm whale click trains: Spectrogram of click trains recorded at Stn 5129 on 1 Sep 2023 (2 Hz discrete Fourier Transform (DFT) frequency step, 0.125 s DFT temporal observation window (TOW), 0.03125 s DFT time advance, and Hann window resulting in a 75 % overlap and DFT size (NDFT) of 256), log scale). The spectrogram is 120 s long.

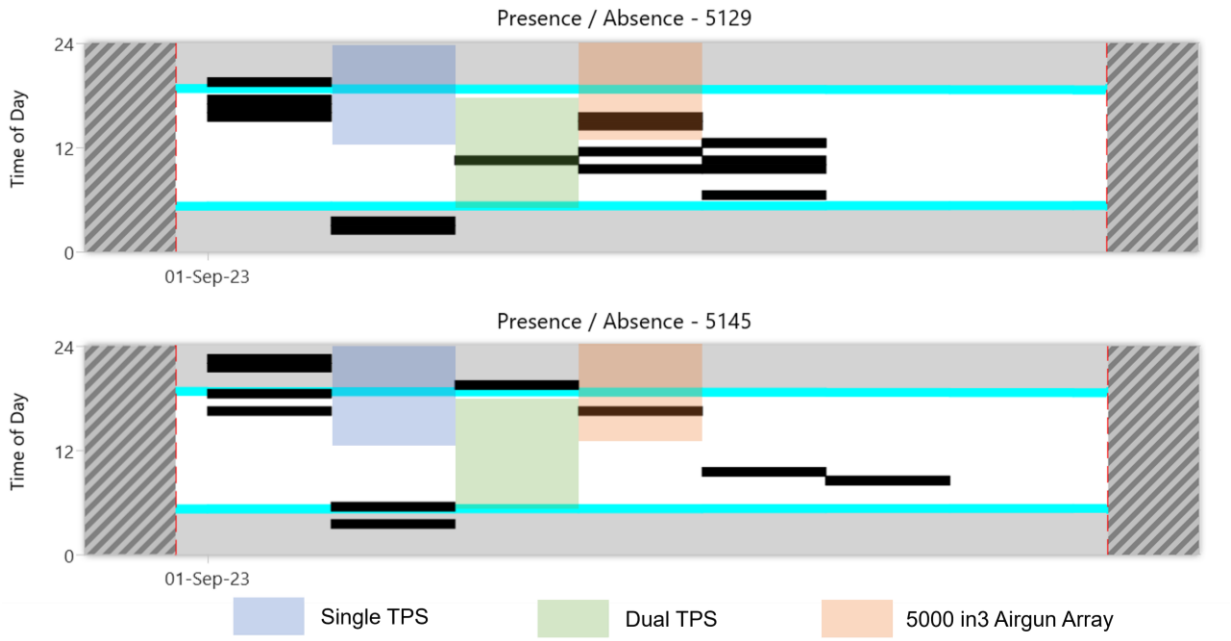

Figure 22. Sperm whale occurrence: Daily and hourly occurrence of clicks recorded at Stn 5129 and Stn 5145 from 1–7 Sep 2023. Black rectangles show manually validated detections. Red dashed lines are the recorder deployment and retrieval dates. Times when each sources was active are overlaid.

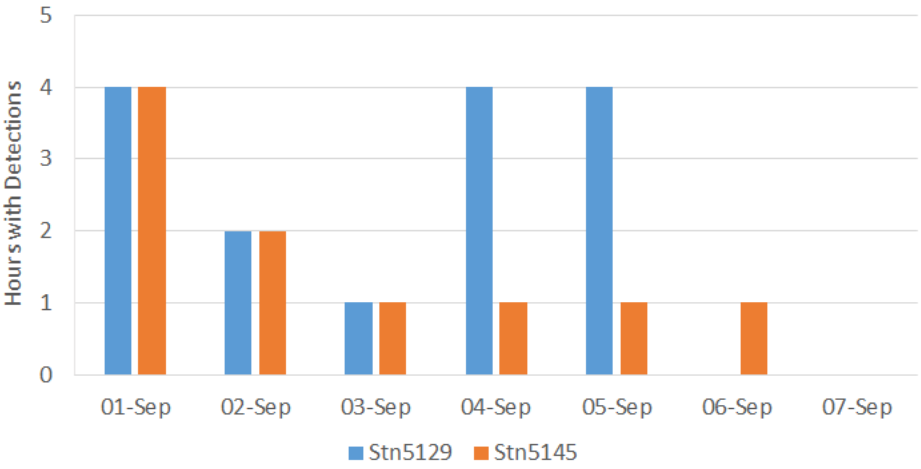

Figure 23. Sperm whale: Number of hours per day containing manual detections at Stn 5129 and Stn 5145.

3.6.3. Delphinids

Unidentified dolphin species (one or more) were detected manually and automatically during the recording period. Both whistles and echolocation were detected (Figure 24). Detections occurred every day, spreading over 2 to 12 h per day (Figures 25 to 27).

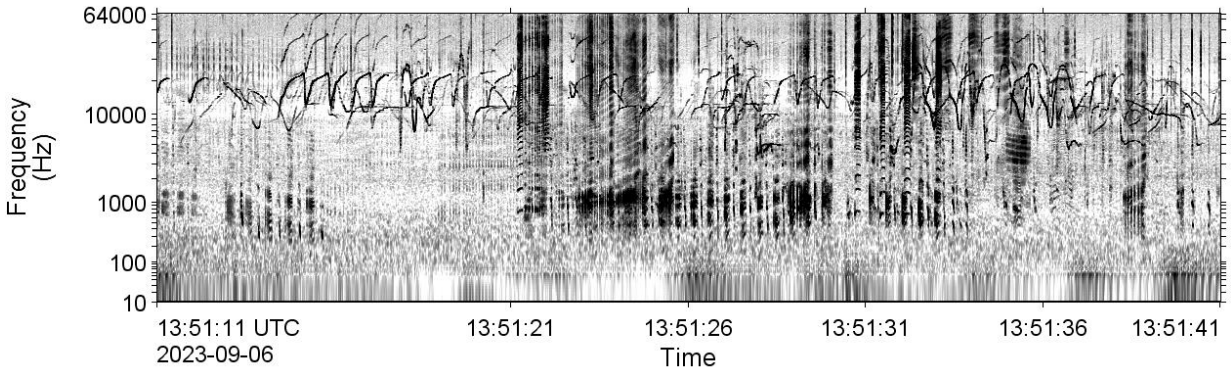

Figure 24. Unidentified dolphin: Spectrogram of unidentified dolphin whistles and click trains recorded at Stn 5145 on 6 Sep 2023 (2 Hz discrete Fourier Transform (DFT) frequency step, 0.125 s DFT temporal observation window (TOW), 0.03125 s DFT time advance, and Hann window resulting in a 75 % overlap and DFT size (NDFT) of 256), log scale). The spectrogram is 30 s long.

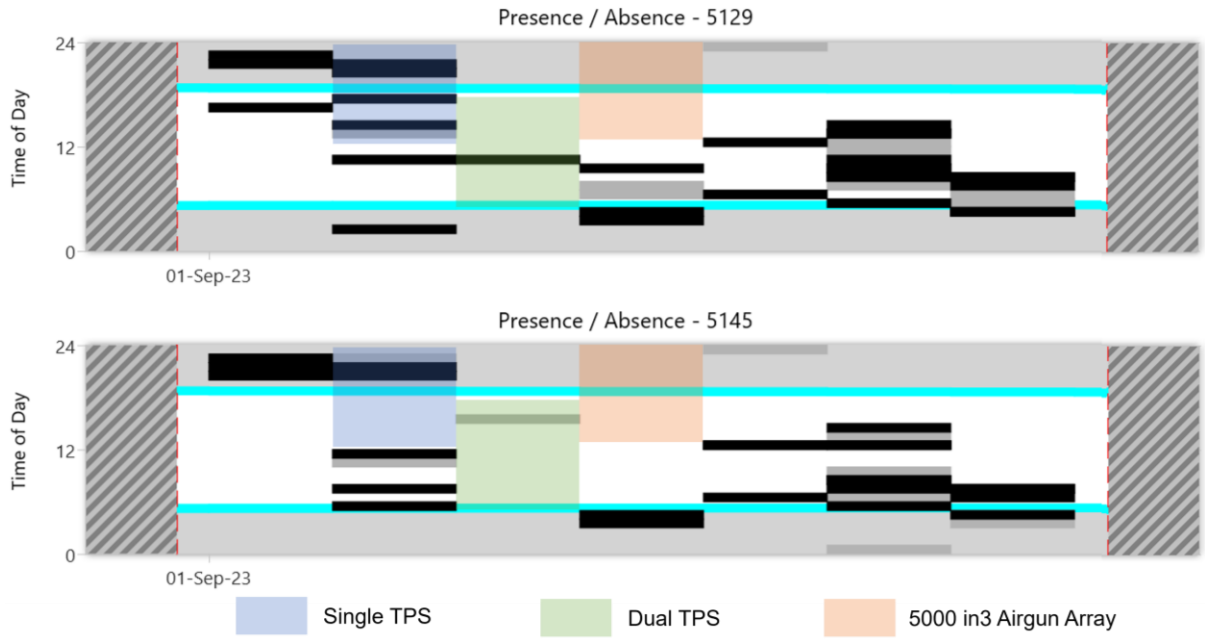

Figure 25. Unidentified dolphin whistle occurrence: Daily and hourly occurrence of whistles recorded at Stn 5129 and Stn 5145 from 1–7 Sep 2023. Grey rectangles are automated detections and black rectangles are manually validated results. Red dashed lines are the recorder deployment and retrieval dates. Times when each sources was active are overlaid.

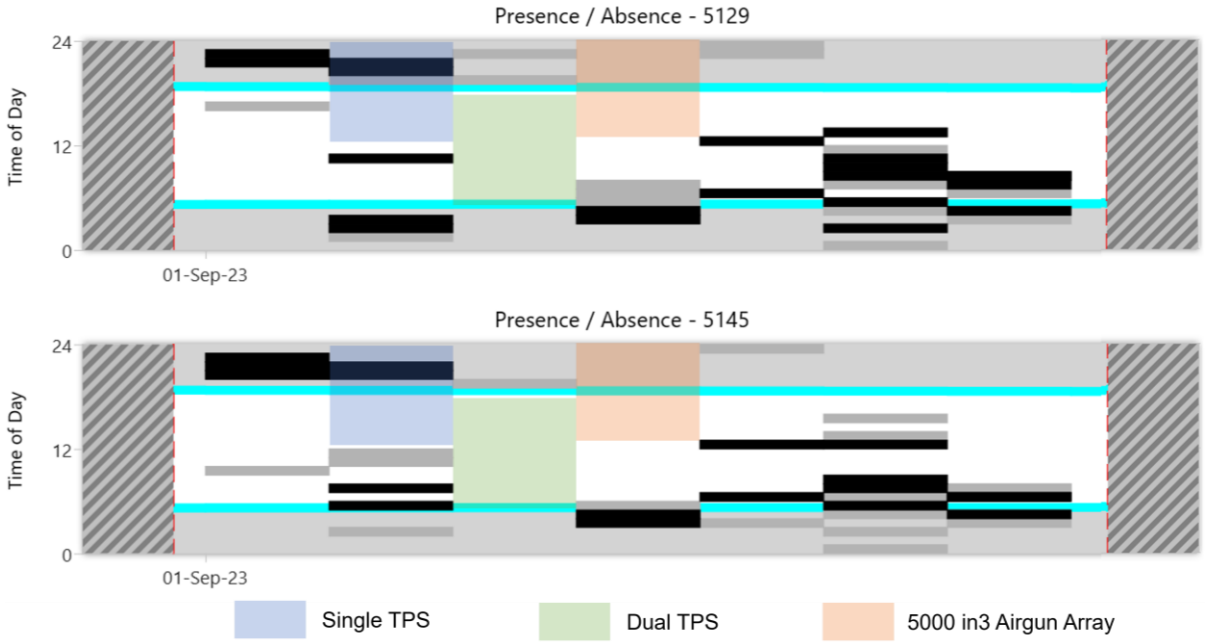

Figure 26. Unidentified dolphin click occurrence: Daily and hourly occurrence of clicks recorded at Stn 5129 and Stn 5145 from 1–7 Sep 2023. Grey rectangles are automated detections and black rectangles are manually validated results. Red dashed lines are the recorder deployment and retrieval dates. Times when each sources was active are overlaid.

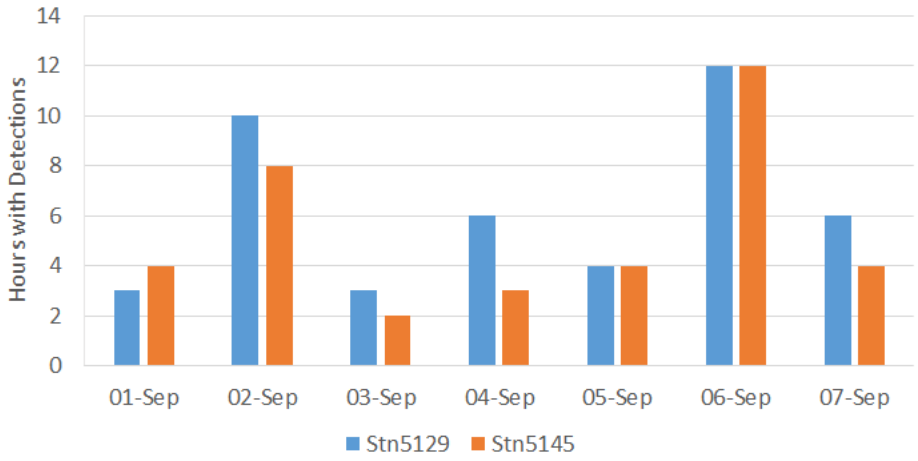

Figure 27. Dolphins: Number of hours per day containing unidentified manual detections (both whistles and clicks) at Stn 5129 and Stn 5145.

4. Discussion and Conclusion

4.1. Background Noise Levels

The measurements were made using moorings with ~350 m ropes extending from the seabed to the hydrophones so that data could be collected at ~100 m water depth. The systems employed coated ropes to reduce flow noise and movement, and currents were expected to be low. However, significant flow noise and movement noise occurred, which were mostly mitigated during processing using a 10 Hz high pass filter that had limited effects on the comparisons between sources when the energy was auditory frequency weighted, which was the primary focus of this analysis. However, when using the M-weightings to assess behavioral reaction distances the noise levels prevented the use of the recorder 5129 data.

If long line moorings must be used in future projects in the Gulf of Mexico, it is recommended that ropes with hairy fairings be employed (Figure 28). These tend to increase the drag on the mooring and require extra flotation to achieve the same hydrophone depths, however they are much more effective at reducing cable strum than the ‘shakedown’ coating employed for this measurement. Streamlined flotation can also be considered for future measurements.



Figure 28. Photo of rope with hairy fairings embedded.

4.2. Measurement Depth Considerations

For many applications it is recommended that recorders always be located on the seabed if the sources of interest are low frequency and currents can cause strum and hydrophone movement noise. However, are seabed measurements suitable for characterizing the risk of sound exposure of marine mammals to seismic sources in deep water? The key measurement is the variation in sound levels as a function of direction around the sound source. Airgun arrays are known to have horizontal and vertical beampatterns. They have higher sound levels directed downwards, and the front-back (endfire) sound levels are often

different than the port-starboard (broadside) sound levels; these effects are shown for the 5000 in^3 array used during these trials in Figures 29 and 30.

To measure a beampattern, measurements must be made at sufficient spatial locations to characterize the pattern. For seismic sources with differences in the horizontal and vertical patterns, a single hydrophone depth cannot measure all angles. Figure 31 uses a contour plot to represent the sampling of a beampattern for a source moving at 2.5 m/s emitting every 20 seconds. The 100-m deep hydrophone is well suited for the horizontal beampattern, while one at 1000 m is better able to measure the vertical beampattern. Both are needed to sample a source that has horizontal and vertical directivity. If a source is more omnidirectional, then either hydrophone will provide sufficient information to understand the output of the source. In airgun arrays, the directivity is due to the geometry of the airguns relative to one another – the larger the array, the more directional it becomes. In the case of a TPS, it does not have multiple elements to generate a beampattern and hence is expected to be much more omnidirectional. For TPS sources, a recording at the seabed is likely sufficient to characterize the source levels.

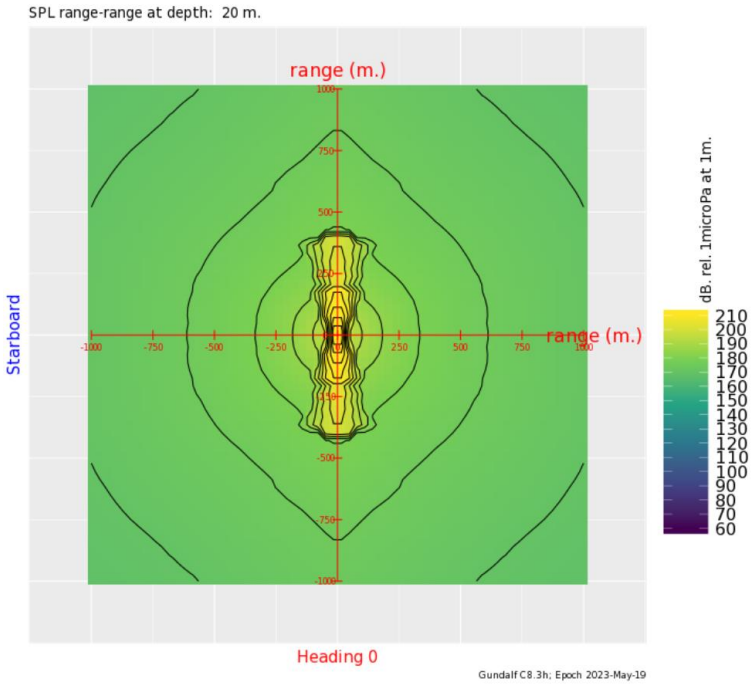

Figure 29. Top-down view of the per-pulse broadband SPL from the 5000 in3 array. Higher sound levels are emitted horizontally at endfire than broadside. From the Gundalf report Gundalf_repC_5000_8m_24331.pdf.

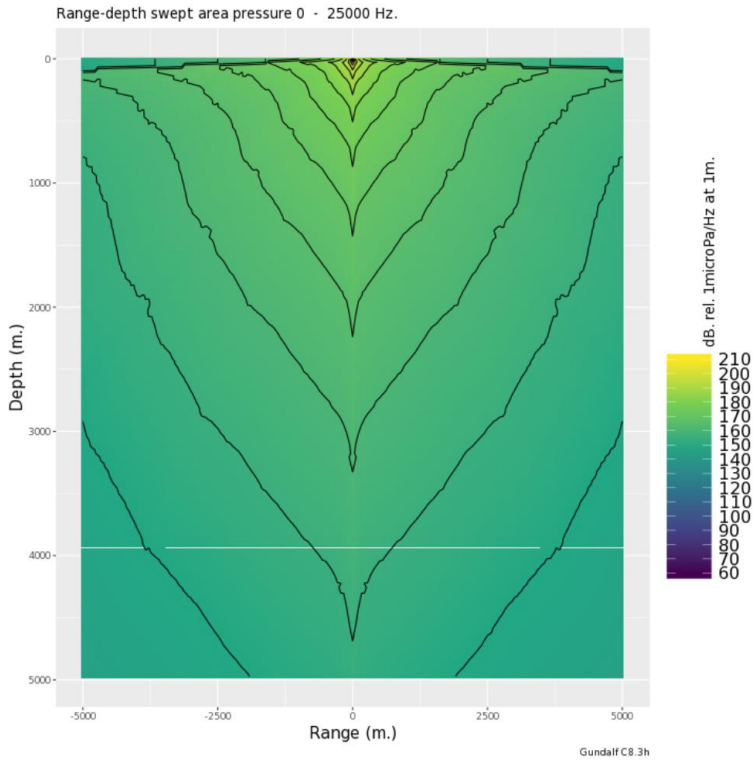

Figure 30. Range-depth cross-sectional view of the per-pulse broadband SPL from the 5000 in3 array. Higher sound levels are emitted downwards. From the Gundalf report Gundalf_repC_5000_8m_24331.pdf

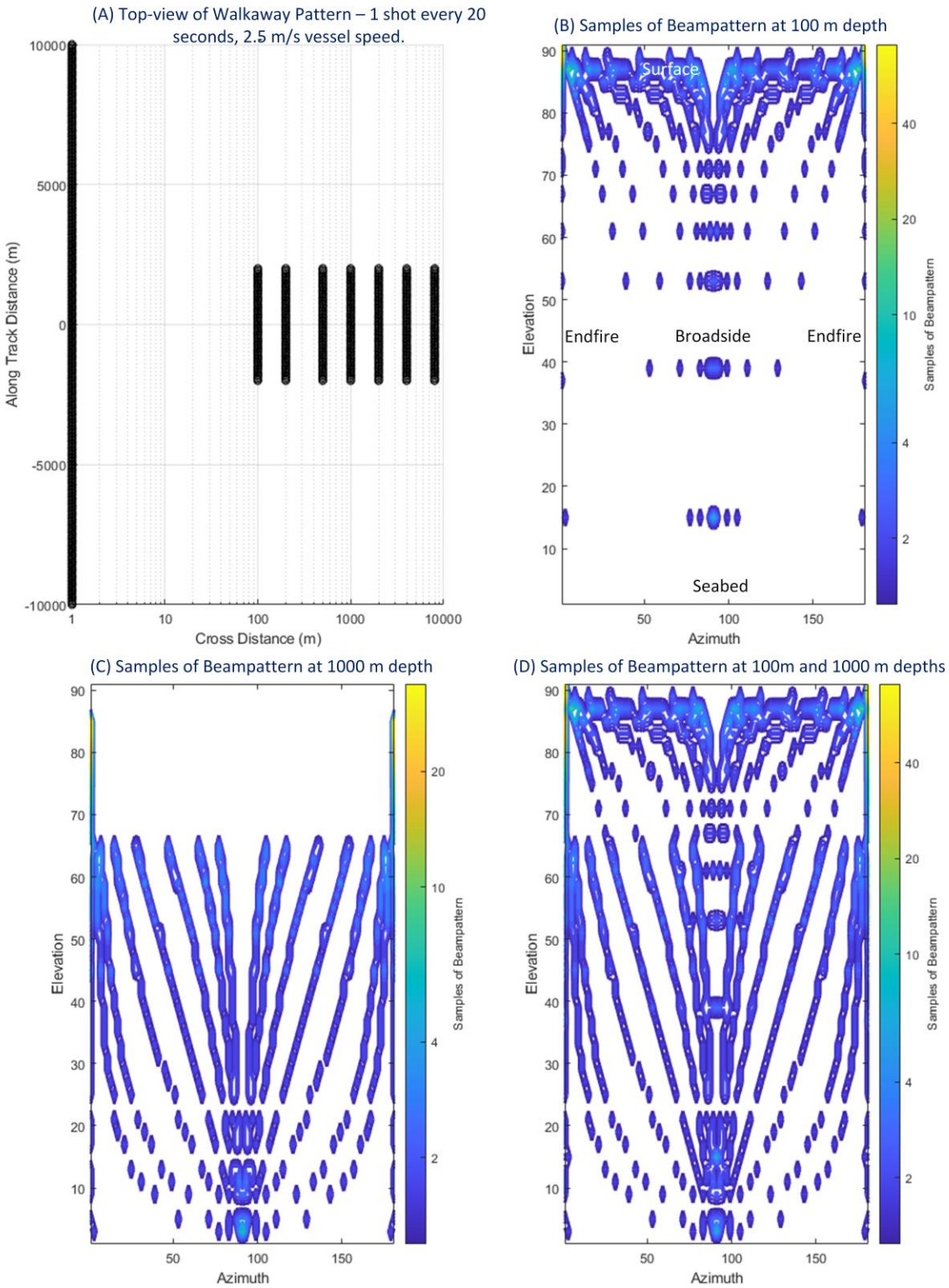

Figure 31. Beampattern sampling for a sound source near the surface following the walkaway pattern shown in (A). The samples from a hydrophone at 100 m depth are shown at (B), at 1000 m at (C) and combining both at (D). In these figures, 0 degrees azimuth is forward endfire, 90 degrees is broadside and 180 is aft endfire. Zero degrees elevation is the sea surface and 90 is the seabed. White cells are not sampled by the vessel tracks.

4.3. Comparison of the Effects of Sound from the Tuned Pulsed Source and Airgun Arrays

This trial allowed for a direct comparison between the received sound levels of a typical airgun array (5000 in^3), and a single or dual tuned pulse source. Assuming the seismic imaging quality of the sources is comparable, the TPS is strongly preferred from a marine mammal sound exposure viewpoint. The sound exposure levels for the dual TPS were 10–14 dB lower for LF mammals, and 28–29 dB lower for HF and VHF mammals. Using an average geometric spreading factor of 20 (see Table 5 and Section 3.4), the 10 dB reduction equates to a 3-fold reduction in exposure distance and 9-fold decrease in exposure area for LF mammals. For the HF and VHF mammals, the distances are reduced by a factor of 25 and the area by a factor of almost 625.

With respect to distances for behavioral disturbance, the shallow water yielded substantially longer disturbance distances in most cases. The distances at which 50 % of the individuals of sensitive species are likely to be disturbed were 5–20 km, while those distances were 1.1 km or less for the less sensitive species such as dolphins and sperm whales. In all cases the distances for the airguns were at least double those for the dual TPS, and the dual TPS distances were greater than for the single TPS.

The percentage of the normal available listening range (ALR) for marine mammals was computed as an index of communication masking. Since seismic pulses are known to reverberate, the amount of time after a pulse that is masked is of interest. The ALR was reduced for 1–2 seconds after the pulse when the source as up to 10 km away, compared to ~5 seconds for the airgun arrays. Substantial masking was found due to the tow vessel. The vessel sounds would cause substantial masking within 5 km for the 80 Hz downsweep of Rice's whales and within ~2 km for the dolphin whistles. Those distance are longer in shallow water than deep.

4.4. Marine Mammals

The marine mammal acoustic detection results presented in this report provide an index of acoustic occurrence for each species. Although acoustic detections can be used to describe the relative abundance of a species across the study area, several factors influence the detectability of the targeted signals. Although an acoustic detection does indicate presence, an absence of detections does not necessarily indicate absence of animals. An animal may be present but not detected if no individuals were vocalizing near the recorder, their signals were masked by environmental and/or anthropogenic noise sources, or a combination of these factors. Different sound propagation environments and different seasonal effects will impact the detection range of a given signal over time and, therefore, influence the number of detectable signals. Seasonal variations in vocalizing behavior may falsely suggest changes in occurrence.

In this study, the lack of baseline data collection prior to the source trials and the strong likelihood of masking, particularly for low frequency sounds such as those of Rice's whales, limited our ability to assess any change in marine mammal occurrence as a result of the activities monitored.

4.4.1. Sperm Whales

Sperm whales are deep diving odontocetes widely distributed in the Gulf of Mexico, including the present study region. Satellite telemetry experiments have shown longitudinal movements along the edge of the continental shelf in the northern Gulf of Mexico but provided no evidence of seasonal movements in this area (Ortega-Ortiz et al. 2012).

Sperm whales were present near both recorders almost daily during the recording period. However, because automated detections could not be used and only 2.8 % of the acoustic data were scanned manually, the results are a minimum estimate of acoustic occurrence. The deployment duration was too short to determine seasonal or temporal patterns of sperm whale vocalizations. Sperm whale clicks were detected more commonly outside of active source times (see Figure 22). This suggests that their clicks may have been masked, changes in their vocalization behavior may have occurred, or the animals avoided the area when sources were active. The proportion of files reviewed for sperm whale clicks was too low to assess any potential effect of the source on the presence of sperm whales. In the absence of automated detections for all recorded sound files, a systematic manual review of the data would be required to assess potential effects of a sound source on sperm whales.

4.4.2. Delphinids

Delphinids known to occur in the study region include Fraser's, bottlenose, Clymene, pantropical spotted, Risso's, rough-toothed, Atlantic spotted, spinner, and striped dolphins (Maze-Foley and Mullin 2006, Würsig 2017). Other delphinid species with similar acoustic signals that are known to occur in the Gulf of Mexico that could be included in the whistle and click detections are short-finned pilot, false, killer, pygmy killer, and melon-headed whales. Identifying the source of the click and whistle detections is difficult based on the limited description of these signals for many of the potential candidate species.

Delphinid vocalizations were detected every day of the recording period. However, they were notably more common outside of active sources times, especially for the dual TPS and 5000 in^3 airgun array sources, which had 2 and 0 detection events, respectively (see Figures 25 and 26). Detections occurred regularly during the single TPS, despite it having similar masking potential to the dual TPS (Figure 20). This could indicate an avoidance of the area after the onset of the trials (single TPS occurred first) or a

change in vocal behavior. Detections appeared to resume after the airgun array trial, but longer pre- and post-trial exposure acoustic data would be needed to assess whether this indicates a return to normal frequentation of the area or acoustic behavior or is consistent with normal patterns of delphinid occurrence in this area.

Literature Cited

[ANSI] American National Standards Institute and [ASA] Acoustical Society of America. S1.1-2013. *American National Standard: Acoustical Terminology*. NY, USA. https://webstore.ansi.org/Standards/ASA/ANSIASAS12013.

[ISO] International Organization for Standardization. 2017. *ISO 18405:2017. Underwater acoustics – Terminology*. Geneva. https://www.iso.org/standard/62406.html.

[NMFS] National Marine Fisheries Service (US). 2018. *2018 Revision to: Technical Guidance for Assessing the Effects of Anthropogenic Sound on Marine Mammal Hearing (Version 2.0): Underwater Thresholds for Onset of Permanent and Temporary Threshold Shifts*. US Department of Commerce, NOAA. NOAA Technical Memorandum NMFS-OPR-59. 167 p. https://media.fisheries.noaa.gov/dam-migration/tech_memo_acoustic_guidance_(20)_(pdf)_508.pdf.

Au, W.W.L., R.A. Kastelein, T. Rippe, and N.M. Schooneman. 1999. Transmission beam pattern and echolocation signals of a harbor porpoise (*Phocoena phocoena*). *Journal of the Acoustical Society of America* 106(6): 3699-3705. https://doi.org/10.1121/1.428221.

Berchok, C.L., D.L. Bradley, and T.B. Gabrielson. 2006. St. Lawrence blue whale vocalizations revisited: Characterization of calls detected from 1998 to 2001. *Journal of the Acoustical Society of America* 120(4): 2340-2354. https://doi.org/10.1121/1.2335676.

Chelminski, S., L.M. Watson, and S. Ronen. 2019. Research Note: Low-frequency pneumatic seismic sources. *Geophysical Prospecting* 67(6): 1547-1556. https://doi.org/10.1111/1365-2478.12774.

Delarue, J.J.-Y., K.A. Kowarski, E.E. Maxner, J.T. MacDonnell, and S.B. Martin. 2018. *Acoustic Monitoring Along Canada's East Coast: August 2015 to July 2017*. Document 01279, Environmental Studies Research Funds Report Number 215, Version 1.0. Technical report by JASCO Applied Sciences for Environmental Studies Research Fund, Dartmouth, NS, Canada. 120 pp + appendices.

Erbe, C., C.J. Reichmuth, K. Cunningham, K. Lucke, and R.J. Dooling. 2016. Communication masking in marine mammals: A review and research strategy. *Marine Pollution Bulletin* 103(1): 15-38. https://doi.org/10.1016/j.marpolbul.2015.12.007.

Erbs, F., S.H. Elwen, and T. Gridley. 2017. Automatic classification of whistles from coastal dolphins of the southern African subregion. *Journal of the Acoustical Society of America* 141(4): 2489-2500. https://doi.org/10.1121/1.4978000.

Finneran, J.J. 2015. *Auditory weighting functions and TTS/PTS exposure functions for cetaceans and marine carnivores*. Technical report by SSC Pacific, San Diego, CA, USA.

Finneran, J.J. 2016. *Auditory weighting functions and TTS/PTS exposure functions for marine mammals exposed to underwater noise*. Technical Report for Space and Naval Warfare Systems Center Pacific, San Diego, CA, USA. 49 p. https://apps.dtic.mil/dtic/tr/fulltext/u2/1026445.pdf.

Hodge, K.B., C.A. Muirhead, J.L. Morano, C.W. Clark, and A.N. Rice. 2015. North Atlantic right whale occurrence near wind energy areas along the mid-Atlantic US coast: Implications for management. *Endangered Species Research* 28(3): 225-234. https://doi.org/10.3354/esr00683.

Kowarski, K.A., J.J.-Y. Delarue, B.J. Gaudet, and S.B. Martin. 2021. Automatic data selection for validation: A method to determine cetacean occurrence in large acoustic data sets. *JASA Express Letters* 1: 051201. https://doi.org/10.1121/10.0004851.

Maze-Foley, K. and K.D. Mullin. 2006. Cetaceans of the oceanic northern Gulf of Mexico: Distributions, group sizes and interspecific associations. *Journal of Cetacean Research and Management* 8(2): 203-213.

Møhl, B., M. Wahlberg, P.T. Madsen, L.A. Miller, and A. Surlykke. 2000. Sperm whale clicks: Directionality and source level revisited. *Journal of the Acoustical Society of America* 107(1): 638-648. https://doi.org/10.1121/1.428329.

Nedwell, J.R. and A.W. Turnpenny. 1998. The use of a generic frequency weighting scale in estimating environmental effect. *Workshop on Seismics and Marine Mammals*. 23–25 Jun 1998, London, UK.

Nedwell, J.R., A.W. Turnpenny, J. Lovell, S.J. Parvin, R. Workman, J.A.L. Spinks, and D. Howell. 2007. *A validation of the dB_{ht} as a measure of the behavioural and auditory effects of underwater noise*. Document 534R1231 Report by Subacoustech Ltd. for Chevron Ltd, TotalFinaElf Exploration UK PLC, Department of Business, Enterprise and Regulatory Reform, Shell UK Exploration and Production Ltd, The Industry Technology Facilitator, Joint Nature Conservation Committee, and The UK Ministry of Defence. 74 p. https://tethys.pnnl.gov/sites/default/files/publications/Nedwell-et-al-2007.pdf.

Ortega-Ortiz, J.G., D. Engelhaupt, M. Winsor, B.R. Mate, and A. Rus Hoelzel. 2012. Kinship of long-term associates in the highly social sperm whale. *Molecular Ecology* 21(3): 732-744.

Pine, M.K., K. Nikolich, S.B. Martin, C. Morris, and F. Juanes. 2020. Assessing auditory masking for management of underwater anthropogenic noise. *Journal of the Acoustical Society of America* 147(5): 3408-3417. https://doi.org/10.1121/10.0001218.

Risch, D., C.W. Clark, P.J. Corkeron, A. Elepfandt, K.M. Kovacs, C. Lydersen, I. Stirling, and S.M. Van Parijs. 2007. Vocalizations of male bearded seals, *Erignathus barbatus*: Classification and geographical variation. *Animal Behaviour* 73(5): 747-762. https://doi.org/10.1016/j.anbehav.2006.06.012.

Širović, A., A. Rice, E. Chou, J.A. Hildebrand, S.M. Wiggins, and M.A. Roch. 2015. Seven years of blue and fin whale call abundance in the Southern California Bight. *Endangered Species Research* 28(1): 61-76. https://doi.org/10.3354/esr00676.

Southall, B.L., A.E. Bowles, W.T. Ellison, J.J. Finneran, R.L. Gentry, C.R. Greene, Jr., D. Kastak, D.R. Ketten, J.H. Miller, et al. 2007. Marine Mammal Noise Exposure Criteria: Initial Scientific Recommendations. *Aquatic Mammals* 33(4): 411-521. https://doi.org/10.1578/AM.33.4.2007.411.

Southall, B.L., J.J. Finneran, C.J. Reichmuth, P.E. Nachtigall, D.R. Ketten, A.E. Bowles, W.T. Ellison, D.P. Nowacek, and P.L. Tyack. 2019. Marine Mammal Noise Exposure Criteria: Updated Scientific Recommendations for Residual Hearing Effects. *Aquatic Mammals* 45(2): 125-232. https://doi.org/10.1578/AM.45.2.2019.125.

Steiner, W.W. 1981. Species-specific differences in pure tonal whistle vocalizations of five western North Atlantic dolphin species. *Behavioral Ecology and Sociobiology* 9(4): 241-246. https://doi.org/10.1007/BF00299878.

Van Parijs, S.M., B.L. Southall, and Convenors and Workshop co-chairs. 2007. *Report of the 2006 NOAA National Passive Acoustics Workshop: Developing a Strategic Program Plan for NOAA's Passive Acoustics Ocean Observing System (PAOOS)*. US Department of Commerce, NOAA Technical Memo NMFS-F/SPO-81, Woods Hole, MA, USA. 64 p. https://spo.nmfs.noaa.gov/sites/default/files/tm81.pdf.

Wood, J.D., B.L. Southall, and D.J. Tollit. 2012. *PG&E offshore 3-D Seismic Survey Project Environmental Impact Report–Marine Mammal Technical Draft Report*. Report by SMRU Ltd. 121 p. https://www.coastal.ca.gov/energy/seismic/mm-technical-report-EIR.pdf.

Würsig, B. 2017. Marine Mammals of the Gulf of Mexico. *In* Ward, C.H. (ed.). *Habitats and Biota of the Gulf of Mexico: Before the Deepwater Horizon Oil Spill: Volume 2: Fish Resources, Fisheries, Sea Turtles, Avian Resources, Marine Mammals, Diseases and Mortalities*. Springer, New York. pp. 1489-1587. https://doi.org/10.1007/978-1-4939-3456-0_5.

Appendix A. Recorder Calibration and Mooring Design

A.1. Recorder Calibrations

Each AMAR was calibrated before deployment and upon retrieval (battery life permitting) with a pistonphone type 42AC precision sound source (G.R.A.S. Sound & Vibration A/S; Figure A-1). The pistonphone calibrator produces a constant tone at 250 Hz at a fixed distance from the hydrophone sensor in an airtight space of known volume. The recorded level of the reference tone on the AMAR yields the system gain for the AMAR and hydrophone. To determine absolute sound pressure levels, this gain was applied during data analysis. Typical calibration variance using this method is less than 0.7 dB absolute pressure.



Figure A-1. Split view of a G.R.A.S. 42AC pistonphone calibrator with an M36 hydrophone.

Appendix B. Acoustic Data Analysis

B.1. Measurement Terminology

Acoustic energy loss due to propagation from the source to receiver depends on the relative distance of the receiver from the source. The slant range is the direct line separation of source and receiver. The horizontal range is the horizontal component of the slant range, as depicted in Figure B-1. The vertical separation between the source and receiver is the water depth minus the source depth and minus the elevation of the hydrophone above the seabed. When the slant range increases to several times the vertical separation, the slant range and horizontal range converge. Slant range is the main distance metric used in this report.

Endfire and broadside are the principal directions in the horizontal plane relative to the acoustic source. The endfire direction is along the tow axis (i.e., fore and aft), and the broadside direction is perpendicular to the tow axis (i.e., port and starboard). Seismic airgun arrays are often directional sources, so the received levels in both the broadside and endfire directions were separately assessed.

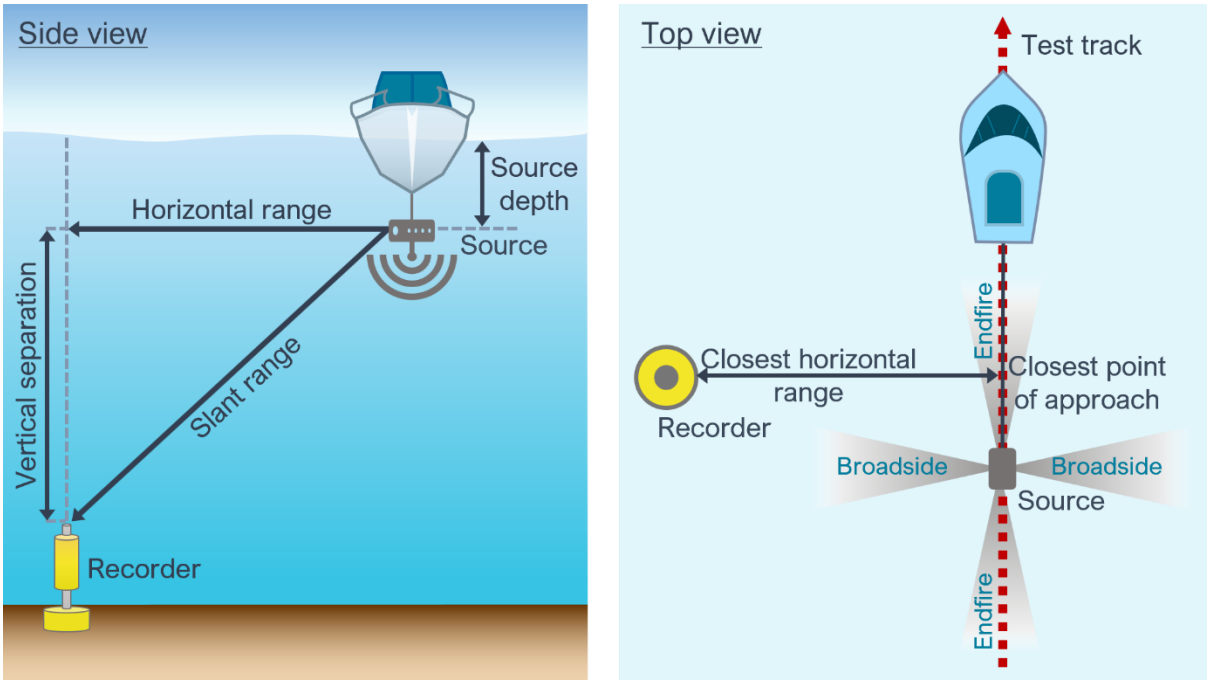

Figure B-1. Typical geometry of sound source characterization (SSC) measurements and the associated terminology used in this report.

B.2. Acoustic Metrics

Underwater sound pressure amplitude is quantified in decibels (dB) relative to a fixed reference pressure of p_0 = 1 µPa. Because the perceived loudness of sound, especially pulsed sound such as from seismic airguns, pile driving, and sonar, is not generally proportional to the instantaneous acoustic pressure, several sound level metrics are commonly used to evaluate sound and its effects on marine life. Here we provide specific definitions of relevant metrics used in the accompanying report. Where possible, we follow International Organization for Standardization definitions and symbols for sound metrics (e.g., ISO 18405:2017, ANSI S1.1-2013).

[zero-to-peak sound pressure (PK)]

The zero-to-peak sound pressure, or peak sound pressure (PK or L_{pk}; dB re 1 µPa), is the decibel level of the maximum instantaneous sound pressure in a stated frequency band attained by an acoustic pressure signal, $p(t)$:

$$L_{\mathrm{pk}} = 10\log_{10}\frac{p_{\mathrm{pk}}^2}{p_0^2} = 20\log_{10}\frac{p_{\mathrm{pk}}}{p_0} = 20\log_{10}\frac{\max|p(t)|}{p_0}. \quad \text{(B-1)}$$

PK is often included as a criterion for assessing whether a sound is potentially injurious; however, because it does not account for the duration of an acoustic event, it is generally a poor indicator of perceived loudness.

[sound pressure level (SPL)]

The sound pressure level (SPL or L_p; dB re 1 µPa) is the root-mean-square (rms) pressure level in a stated frequency band over a specified time window (T; s):

$$L_p = 10\log_{10}\frac{p_{\mathrm{rms}}^2}{p_0^2} = 10\log_{10}\left(\frac{1}{T}\int_T p^2(t)\,dt \Big/ p_0^2\right). \quad \text{(B-2)}$$

It is important to note that SPL always refers to an rms pressure level (i.e., a quadratic mean over a time interval) and therefore not instantaneous pressure at a fixed point in time. The SPL can also be defined as the *mean-square* pressure level, given in decibels relative to a reference value of 1 µPa^2 (i.e., in dB re 1 µPa^2). The two definitions of SPL are numerically equivalent, differing only in reference value.

[Time-weighted SPL]

The SPL can also be calculated using a time weighting function, $g(t)$:

$$L_p = 10\log_{10}\left(\frac{1}{T}\int_T g(t)\,p^2(t)\,dt \Big/ p_0^2\right) \text{ dB} \quad \text{(B-3)}$$

In many cases, the start time of the integration is marched forward in small time steps to produce a time-varying SPL function. For short acoustic events, such as sonar pulses and marine mammal vocalizations, it is important to choose an appropriate time window that matches the duration of the signal. For in-air studies, when evaluating the perceived loudness of sounds with rapid amplitude variations in time, the time weighting function $g(t)$ is often set to a decaying exponential function that emphasizes more recent pressure signals. This function mimics the leaky integration nature of mammalian hearing. For example, human-based fast time-weighted SPL ($L_{p,\mathrm{fast}}$) applies an exponential function with time constant 125 ms. A

related simpler approach used in underwater acoustics sets $g(t)$ to a boxcar (unity amplitude) function of width 125 ms; the results can be referred to as $L_{p,\text{boxcar 125ms}}$.

[90 % Duration SPL]

Another approach, historically used to evaluate SPL of impulsive signals underwater (e.g., from pile driving or seismic airguns), defines $g(t)$ as a boxcar function with edges set to the times corresponding to 5 % and 95 % of the cumulative square pressure function encompassing the duration of an impulsive acoustic event. This calculation is applied individually to each impulse signal, and the results have been referred to as 90 % SPL ($L_{p,90}$).

[sound exposure level (SEL)]

The sound exposure level (SEL or L_E; dB re 1 µPa^2 s) is the time-integral of the squared acoustic pressure over a duration (T):

$$L_E = 10 \log_{10} \left(\int_T p^2(t)\, dt \Big/ T_0 p_0^2 \right) \text{dB}\,, \tag{B-4}$$

where T_0 is a reference time interval of 1 s. SEL continues to increase with time when non-zero pressure signals are present. It is a dose-type measurement, so the integration time applied must be carefully considered for its relevance to impact to the exposed recipients. SEL can be calculated over a fixed duration, such as the time of a single event or a period with multiple acoustic events.

[Relating SPL and SEL]

Because the SPL and SEL are both computed from the integral of square pressure, these metrics are related numerically by the following expression, which depends only on the duration of the time window T:

$$L_p = L_E - 10\log_{10}(T)\,. \tag{B-5}$$

[Relating SPL(T_{90}) and SEL]

Likewise, the SPL(T_{90}) and SEL metrics are related by:

$$L_{p,90} = L_E - 10\log_{10}(T_{90}) - 0.458\,, \tag{B-6}$$

where the 0.458 dB factor accounts for the 10 % of pulse SEL missing from the SPL(T_{90}) integration time window.

B.3. Decidecade Band Analysis

The distribution of a sound's power with frequency is described by the sound's spectrum. The sound spectrum can be split into a series of adjacent frequency bands. Splitting a spectrum into 1 Hz wide bands, called passbands, yields the power spectral density of the sound. This splitting of the spectrum into passbands of a constant width of 1 Hz, however, does not represent how animals perceive sound.

Animals perceive exponential increases in frequency rather than linear increases, so analyzing a sound spectrum with passbands that increase exponentially in size better approximates real-world scenarios. In underwater acoustics, a spectrum is commonly split into decidecade bands, which are one tenth of a decade wide. A decidecade is sometimes referred to as a "1/3-octave" because one tenth of a decade is approximately equal to one third of an octave. Each decade represents a factor of 10 in sound frequency. Each octave represents a factor of 2 in sound frequency. The center frequency of the ith decidecade band, $f_c(i)$, is defined as:

$$f_{\mathrm{c}}(i) = 10^{\frac{i}{10}}\ \mathrm{kHz}\,, \tag{B-7}$$

and the low (f_{lo}) and high (f_{hi}) frequency limits of the ith decidecade band are defined as:

$$f_{\mathrm{lo},i} = 10^{\frac{-1}{20}} f_{\mathrm{c}}(i) \text{ and } f_{\mathrm{hi},i} = 10^{\frac{1}{20}} f_{\mathrm{c}}(i)\,. \tag{B-8}$$

The decidecade bands become wider with increasing frequency, and on a logarithmic scale the bands appear equally spaced (Figure B-2).

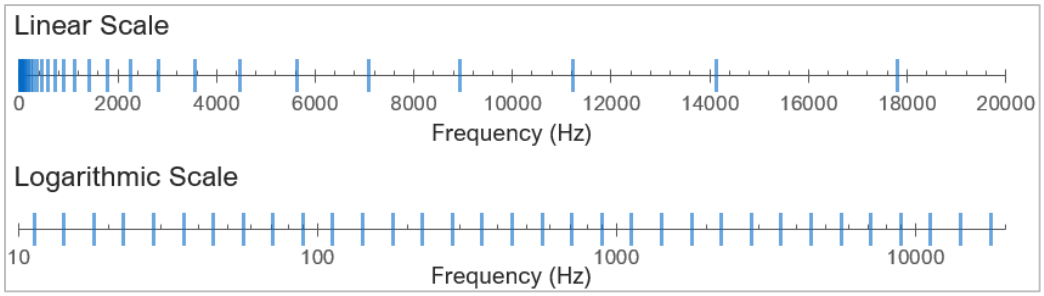

Figure B-2. Decidecade frequency bands (vertical lines) shown on (top) a linear frequency scale and (bottom) a logarithmic scale. On the logarithmic scale, the bands are equally spaced.

The sound pressure level in the ith band ($L_{p,i}$) is computed from the spectrum $S(f)$ between $f_{lo,i}$ and $f_{hi,i}$:

$$L_{p,i} = 10 \log_{10} \int_{f_{\mathrm{lo},i}}^{f_{\mathrm{hi},i}} S(f)\,\mathrm{d}f\ \mathrm{dB}\,. \tag{B-9}$$

Summing the sound pressure level of all the bands yields the broadband sound pressure level:

$$\text{Broadband SPL} = 10 \log_{10} \sum_i 10^{\frac{L_{p,i}}{10}}\ \mathrm{dB}\,. \tag{B-10}$$

Figure B-3 shows an example of how the decidecade band sound pressure levels compare to the sound pressure spectral density levels of an ambient sound signal. Because the decidecade bands are wider than 1 Hz, the decidecade band SPL is higher than the spectral levels at higher frequencies. Decidecade

band analysis can be applied to continuous and impulsive sound sources. For impulsive sources, the decidecade band SEL is typically reported.

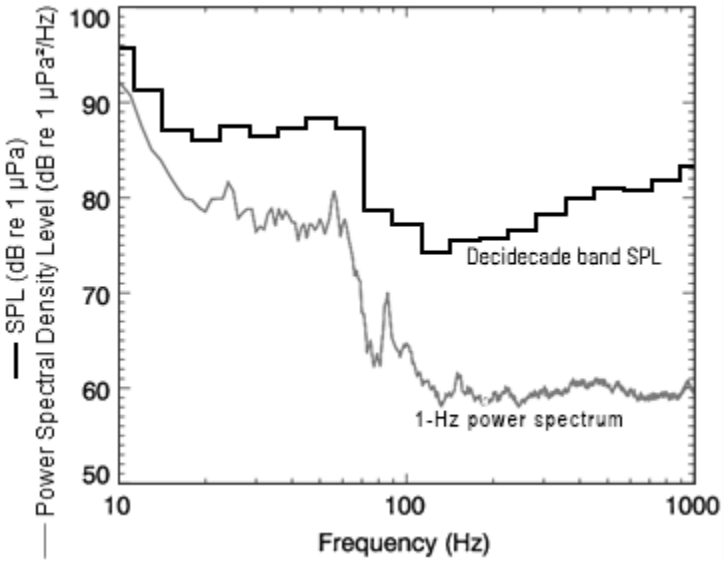

Figure B-3. Sound pressure spectral density levels and the corresponding decidecade band sound pressure levels of example ambient sound shown on a logarithmic frequency scale. Because the decidecade bands are wider with increasing frequency, the decidecade band SPL is higher than the power spectrum, which is based on bands with a constant width of 1 Hz.

Table B-1. Decidecade band center and limiting frequencies (Hz).

Band	Lower frequency	Nominal center frequency	Upper frequency	Band	Lower frequency	Nominal center frequency	Upper frequency
10	8.9	10.0	11.2	26	355	398	447
11	11.2	12.6	14.1	27	447	501	562
12	14.1	15.8	17.8	28	562	631	708
13	17.8	20.0	22.4	29	708	794	891
14	22.4	25.1	28.2	30	891	1000	1122
15	28.2	31.6	35.5	31	1122	1259	1413
16	35.5	39.8	44.7	32	1413	1585	1778
17	44.7	50.1	56.2	33	1778	1995	2239
18	56.2	63.1	70.8	34	2239	2512	2818
19	70.8	79.4	89.1	35	2818	3162	3548
20	89.1	100.0	112.2	36	3548	3981	4467
21	112	126	141	37	4467	5012	5623
22	141	158	178	38	5623	6310	7079
23	178	200	224	39	7079	7943	8913
24	224	251	282	40	8913	10000	11220
25	282	316	355	41	11220	12589	14125

Table B-2. Decade band center and limiting frequencies (Hz).

Decade band	Lower frequency	Nominal center frequency	Upper frequency
2	10	50	100
3	100	500	1000
4	1,000	5,000	10,000

B.4. Marine Mammal Auditory Frequency Weighting

The potential for noise to affect animals depends on how well the animals can hear it. Noises are less likely to disturb or injure an animal if the noises are at frequencies that the animal cannot hear well. An exception occurs when the sound pressure is so high that it can physically injure an animal by non-auditory means (i.e., barotrauma). For sound levels below such extremes, the importance of sound components at particular frequencies can be scaled by frequency weighting relevant to an animal's sensitivity to those frequencies (Nedwell and Turnpenny 1998, Nedwell et al. 2007, Van Parijs et al. 2007, Southall et al. 2019).

In 2015, a US Navy technical report by Finneran (2015) recommended new auditory weighting functions. The auditory weighting functions for marine mammals are applied in a similar way as A-weighting for noise level assessments for humans. The new frequency-weighting functions are expressed as:

$$G(f) = K + 10\log_{10}\left\{\frac{(f/f_1)^{2a}}{[1+(f/f_1)^2]^a[1+(f/f_2)^2]^b}\right\} \quad \text{(B-11)}$$

Finneran (2015) proposed five functional hearing groups for marine mammals in water: low-, mid- and high-frequency cetaceans (LF, MF, and HF cetaceans, respectively), phocid pinnipeds, and otariid pinnipeds. The parameters for these frequency-weighting functions were further modified the following year (Finneran 2016) and were adopted in US National Oceanic and Atmospheric Administration's (NOAA's) technical guidance that assesses acoustic impacts on marine mammals (NMFS 2018), and in the latest guidance by Southall et al (2019). The updates did not affect the content related to either the definitions of frequency-weighting functions or the threshold values, however the group naming did change, with the mid and high-frequency cetacean groups from NMFS (2018) being referred to as high and very-high frequency cetaceans in Southall et al (2019). The Southall et al (2019) naming convention is used here. Table B-3 lists the frequency-weighting parameters for each hearing group and shows the resulting frequency-weighting curves.

Table B-3. Parameters for the auditory weighting functions recommended by Southall et al (2019).

Functional hearing group	a	b	f_1 (Hz)	f_2 (Hz)	K (dB)
Low-frequency cetaceans	1.0	2	200	19,000	0.13
High-frequency cetaceans	1.6	2	8,800	110,000	1.20
Very-high-frequency cetaceans	1.8	2	12,000	140,000	1.36
Phocid pinnipeds in water	1.0	2	1,900	30,000	0.75
Otariid pinnipeds in water	2.0	2	940	25,000	0.64

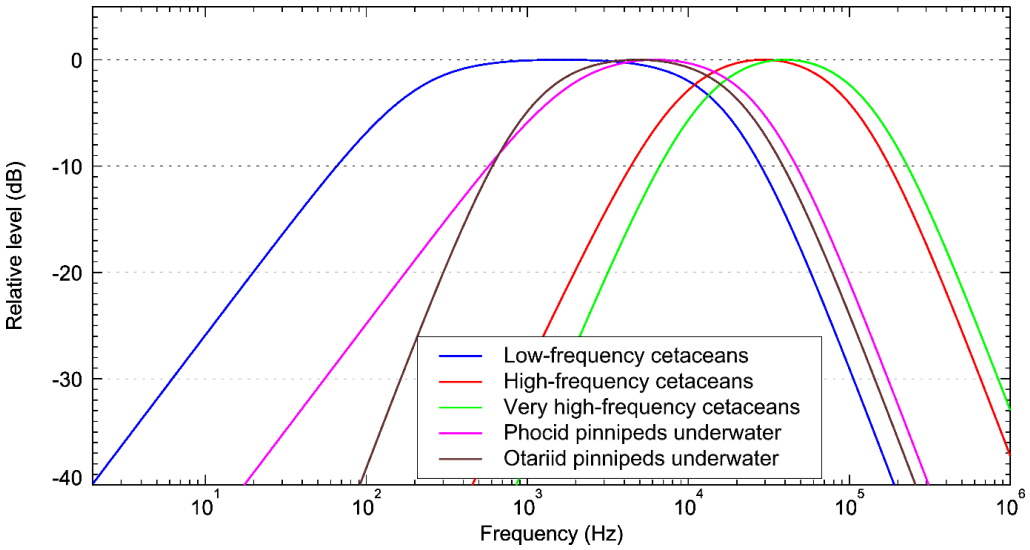

Figure B-4. Auditory weighting functions for the functional marine mammal hearing groups as recommended by Southall (2019).

B.4.1. Southall et al. (2007) Frequency Weighting Functions

Auditory weighting functions for marine mammals called M-weighting functions, were proposed by Southall et al. (2007). These M-weighting functions are applied in a similar way as A-weighting for noise level assessments for humans in air. Functions were defined for four hearing groups of marine mammals in water:

- Low-frequency (LF) cetaceans—mysticetes (baleen whales),
- Mid-frequency (MF) cetaceans—some odontocetes (toothed whales),
- High-frequency (HF) cetaceans—odontocetes specialized for using high-frequencies,
- Pinnipeds in water (Pw)—seals, sea lions, and walrus, and

The M-weighting functions have unity gain (0 dB) through the passband and their high- and low-frequency roll-offs are approximately –12 dB per octave. The amplitude response in the frequency domain of each M-weighting function is defined by:

$$G(f) = -20\log_{10}\left[\left(1+\frac{a^2}{f^2}\right)\left(1+\frac{f^2}{b^2}\right)\right] \quad \text{(B-12)}$$

where $G(f)$ is the weighting function amplitude (in dB) at the frequency f (in Hz), and a and b are the estimated lower and upper hearing limits, respectively, which control the roll-off and passband of the weighting function. The parameters a and b are defined uniquely for each hearing group (Table B-4). Figure B-5 shows the auditory weighting functions recommended by Southall et al. (2007). These weighting functions have been superceded by those in NMFS (2018) and Southall et al (2019) for assessing auditory injury in marine mammals, however, they remain recommended for filtering the spectrum of a signal before assessing behavioral disturbance.

Table B-4. Parameters for the auditory weighting functions recommended by Southall et al. (2007). The pinnipeds in air group has been omitted since it is not relevant to this report.

Functional hearing group	a (Hz)	b (Hz)
Low-frequency cetaceans	7	22,000
Mid-frequency cetaceans	150	160,000
High-frequency cetaceans	200	180,000
Pinnipeds in water	75	75,000

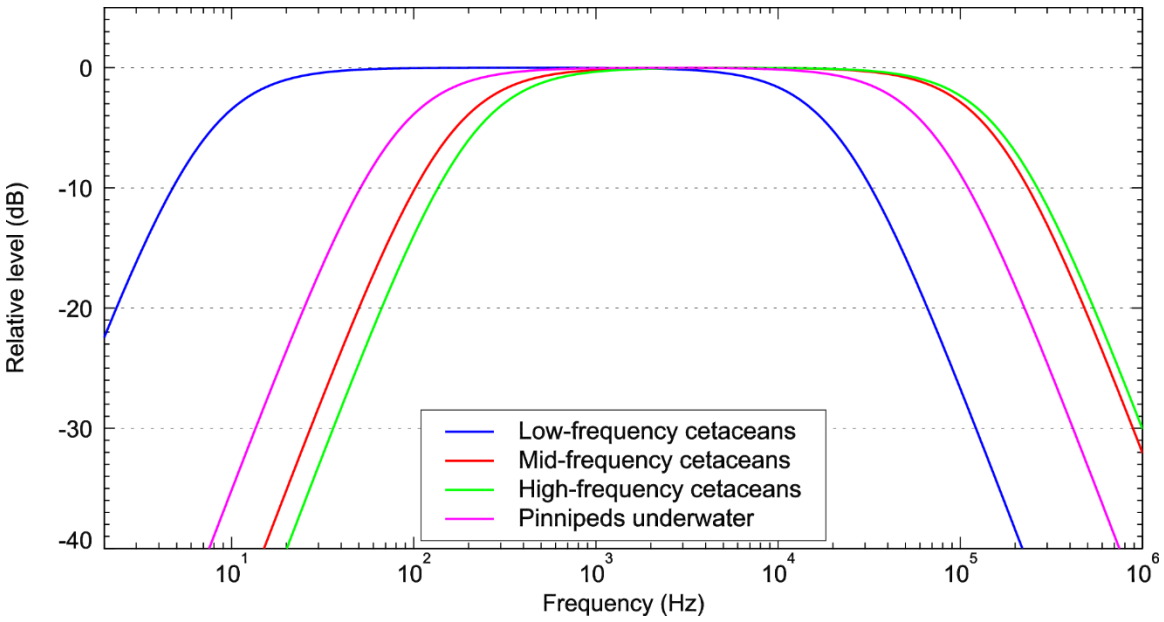

Figure B-5. Auditory weighting functions for the functional marine mammal hearing groups as recommended by Southall et al. (2007). The pinnipeds in air group has been omitted since it is not relevant to this report.

Appendix C. Marine Mammal Detection Methodology

C.1. Automated Click Detector for Odontocetes

Figure C-1 shows how we apply an automated click detector/classifier to the data to detect clicks from odontocetes. This detector/classifier is based on the zero-crossings in the acoustic time series. Zero-crossings are the rapid oscillations of a click's pressure waveform above and below the signal's normal level. Clicks are detected by the following steps:

1. The raw data are high-pass filtered to remove all energy below 5 kHz. This removes most energy from sources other than odontocetes (such as shrimp, vessels, wind, and cetacean tonal calls) yet allows the energy from all marine mammal click types to pass.
2. The filtered samples are summed to create a 0.334 ms rms time series. Most marine mammal clicks have a 0.1–1 ms duration.
3. Possible click events are identified with a split-window normalizer that divides the 'test' bin of the time series by the mean of the 6 'window' bins on either side of the test bin, leaving a 'notch' that is 1-bin wide.
4. A Teager-Kaiser energy detector identifies possible click events.
5. The high-pass filtered data are searched to find the maximum peak signal within 1 ms of the detected peak.
6. The high-pass filtered data are searched backwards and forwards to find the time span when the local data maxima are within 9 dB of the maximum peak. The algorithm allows for two zero-crossings to occur where the local peak is not within 9 dB of the maximum before stopping the search. This defines the time window of the detected click.
7. The classification parameters are extracted. The number of zero crossings within the click, the median time separation between zero crossings, and the slope of the change in time separation between zero-crossings are computed. The slope parameter helps identify beaked whale clicks, because beaked whales can be identified by the increase in frequency (upsweep) of their clicks.
8. The Mahalanobis distance between the extracted classification parameters and the templates of known click types is computed. The covariance matrices for the known click types (computed from thousands of manually identified clicks for each species) are stored in an external file. Each click is classified as a type with the minimum Mahalanobis distance unless none of them are less than the specified distance threshold.

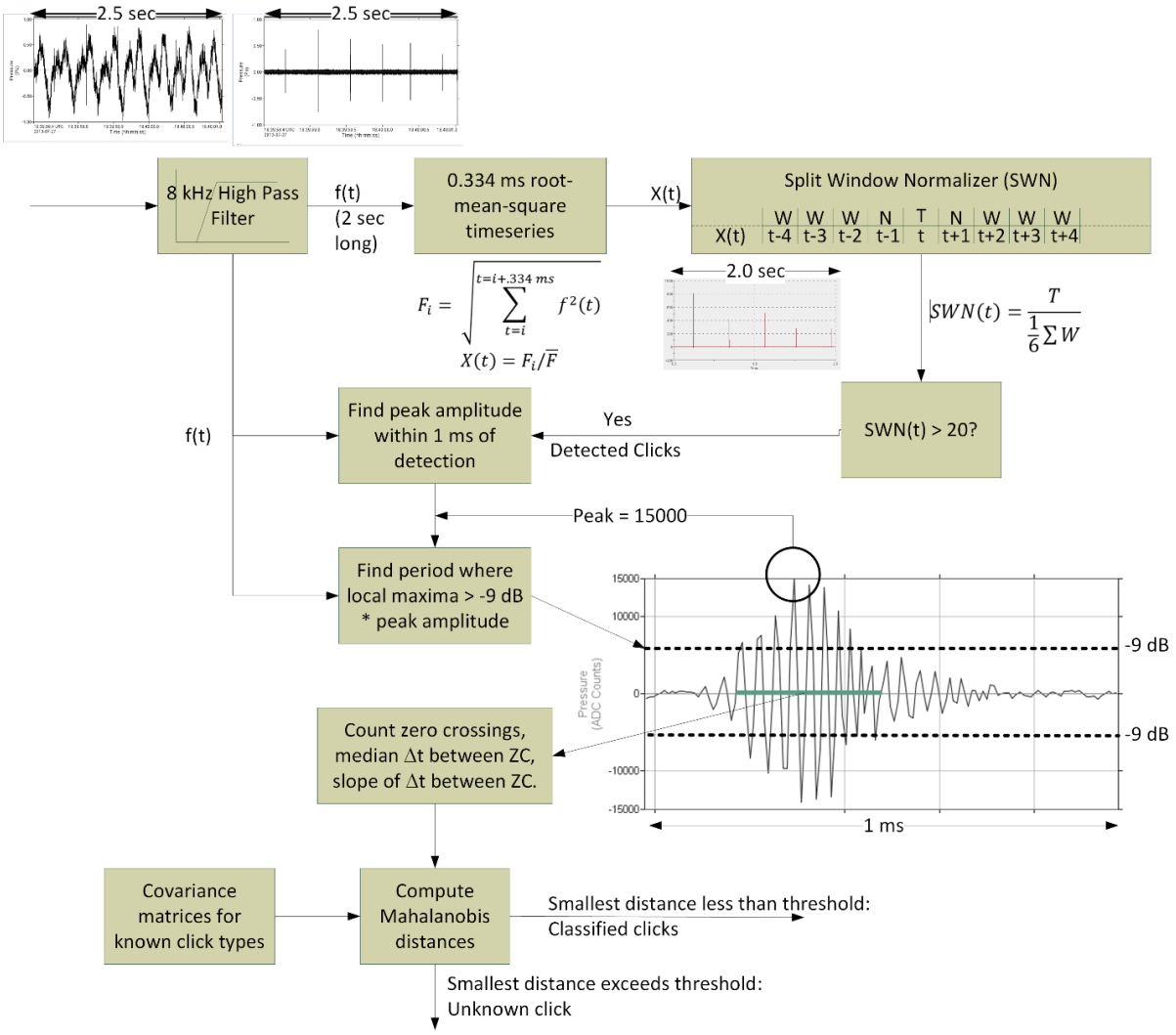

Figure C-1. Flowchart of the automated click detector/classifier process.

Odontocete clicks occur in groups called click trains. Each species has a characteristic inter-click-interval (ICI) and number of clicks per train. The automated click detector includes a second stage that associates individual clicks into trains (Figure C-2). The click train algorithm performs the following steps:

1. Queue clicks for N seconds, where N is twice the maximum number of clicks per train times the maximum ICI.
2. Search for all clicks within the window that have Mahalanobis distances less than 11 for a species of interest (this finds 80 % of all clicks for the species as defined by the template).
3. Create a candidate click train if:
   a. The number of clicks is greater or equal to the minimum number of clicks in a train;
   b. The maximum time between any two clicks is less than 2.5 times the maximum ICI, and
   c. The smallest Mahalanobis distance for all clicks in the candidate train is less than 4.1.
4. Create a new ‘time series’ with a value of 1 at the time of arrival for each click and zero everywhere else (using a ‘time series’ with a bin duration of 0.5 ms).

5. Apply a Hann window to the time series, and then compute the cepstrum.
6. A click train is classified if a peak in the cepstrum with an amplitude greater than five times the standard deviation of the cepstrum occurs at a quefrency between the minimum maximum ICI.
7. For each click related to the previous Ncepstrum, create a new time series and compute ICI. If there is a good match, then extend the click train.
8. Output a species_click_train detection if the click features, total clicks, and mean ICI match the species.

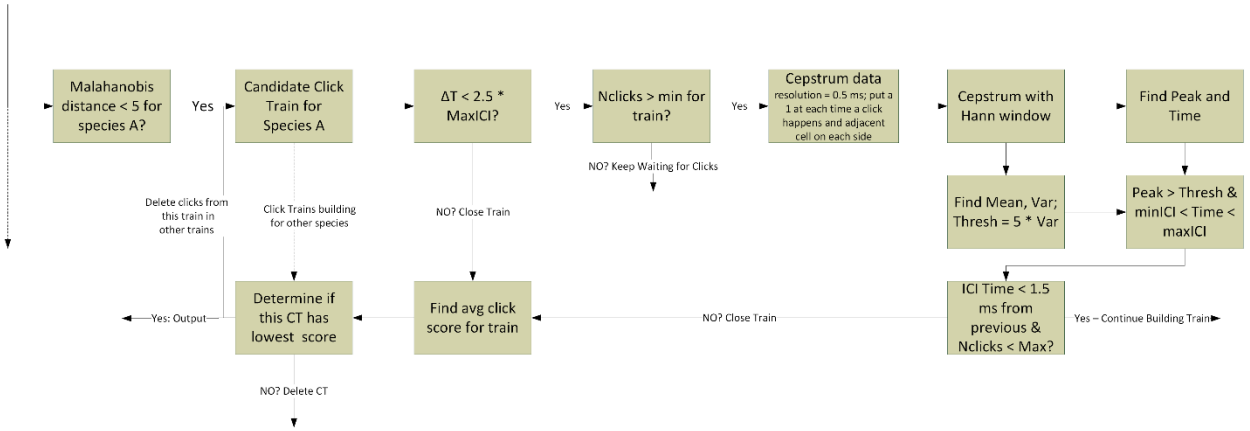

Figure C-2. Flowchart of the click train automated detector/classifier process.

Table C-1. List of automated detectors used to identify clicks produced by odontocetes.

Detector	Species targeted	Detector label		Comments
		Clicks	Click trains	
DefaultClicks_LF.xml	Sperm whale	SpermWhale:Click	SpermWhale (Click Train)	5 kHz HPF
	Killer whale	KillerWhale:Click	KillerWhale (Click Train)	
DefaultClicks_MF.xml	True's or Gervais beaked whale	TBW_GBW:Click	TBW_GBW (Click Train)	25 kHz HPF
	Cuvier's beaked whale	Cuviers:Click	Cuviers (Click Train)	
	Unidentified beaked whale	BW-STP:Click	BW-STP (Click Train)	
	Northern bottlenose whale	NBW:Click	NBW (Click Train)	
	Delphinids	Dolphin:Click	Dolphin (Click Train)	
	Atlantic white-sided dolphin	AWSD_La:Click	AWSD_La (Click Train)	
	Stenella species	StenellaSP:Click	StenellaSP (Click Train)	
	Unidentified dolphin, type A	UDA:Click	UDA (Click Train)	
	Unidentified dolphin, type B	UDB:Click	UDB (Click Train)	
	Pilot whale	PilotWhale:Click	PilotWhale (Click Train)	
	Blainville's beaked whale	Blainsvilles:Click	Blainsvilles (Click Train)	
DefaultClicks_HF.xml	Sowerby's beaked whale	Sowerbys:Click	Sowerbys (Click Train)	50 kHz HPF
	Harbor porpoise/NBHF	Porpoise:Click	Porpoise (Click Train)	
		Porpoise250ksps:Click	Porpoise250ksps (Click Train)	
	Kogiids/NBHF	KSima:Click	KSima (Click Train)	

NBHF = narrow-band high-frequency; HPF = high-pass filter

C.2. Automated Tonal Signal Detection

Marine mammal tonal acoustic signals are automatically detected using the contour detection and following algorithm depicted in Figure C-3. The algorithm has the following steps:

1. Create spectrograms of the appropriate resolution for each mammal vocalization type that were normalized by the median value in each frequency bin for each detection window (Table C-2).
2. Join adjacent bins and create contours via a contour-following algorithm (Figure C-4).
3. Apply a sorting algorithm to determine if the contours match the definition of a marine mammal vocalization (Table C-3).

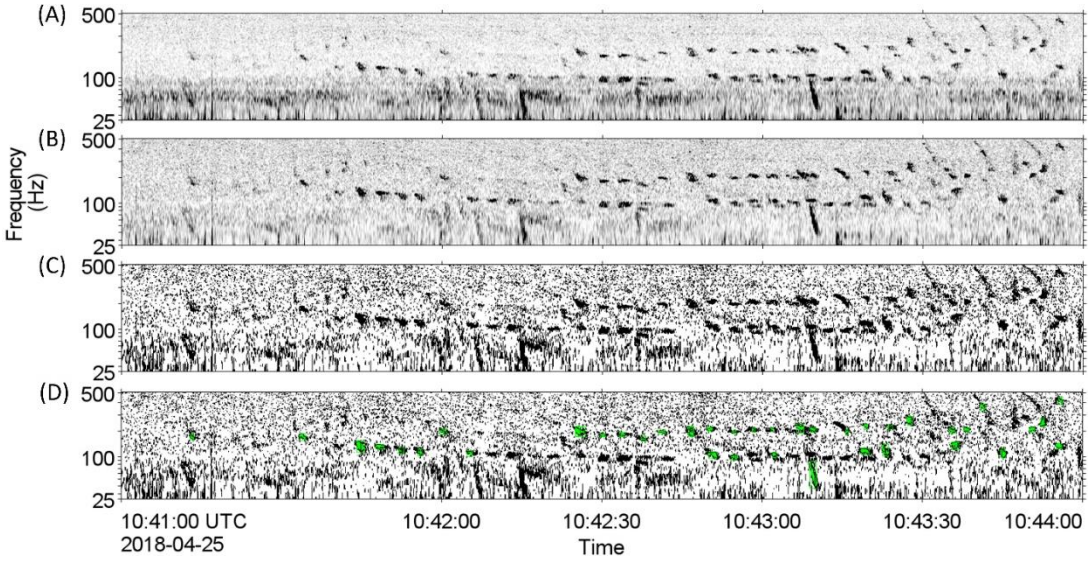

Figure C-3. Illustration of the contour detection process. (A) A spectrogram is generated at the frequency and time resolutions appropriate for the tonal calls of interest. (B) A median normalizer is applied at each frequency. (C) The data are turned into a binary representation by setting all normalized values less than the threshold to 0 and all values greater than the threshold to 1. (D) The regions that are '1' in the binary spectrogram are connected to create contours, which are then sorted to detect signals of interest, shown here as green overlays.

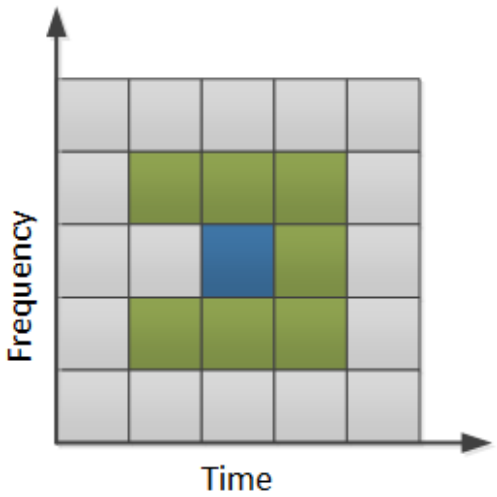

Figure C-4. Illustration of the search area used to connect spectrogram bins. The blue square represents a bin of the binary spectrogram equaling 1, and the green squares represent the potential bins it could be connected to. The algorithm advances from left to right, so grey cells left of the test cell need not be checked.

The tonal signal detector is expanded into a pulse train detector through the following steps:

1. Detect and classify contours as described in Steps 1 and 2 above.
2. A sorting algorithm determines if any series of contours can be assembled into trains that match a pulse train template (Table C-3).

Table C-2. Fast Fourier Transform (FFT) and detection window settings for all automated contour-based detectors used to detect tonal vocalizations of marine mammal species expected in the data. Values are based on JASCO's experience and empirical evaluation of various data sets.

Species targeted	Automated detector	Signal targeted	Discrete Fourier transform			Detection window (s)	Detection threshold
			Frequency step (Hz)	Temporal observation window (s)	Time advance (s)		
Humpback whale, Rice's whale	MFMoanLow	Moan	4	0.2	0.05	5	3
	MFMoanLow_LT		4	0.2	0.05	5	5
Small dolphins	WhistleHigh_Suppress	Whistle with energy between 4–20 kHz	64	0.015	0.005	10	1.5
	WhistleHigh_Quiet		64	0.015	0.005	10	1.5
	WhistleHigh_Loud		64	0.015	0.005	10	4.5
Pilot, killer whale	WhistleLow_Suppress	Whistle with energy between 1–10 kHz	8	0.125	0.05	10	1.5
	WhistleLow_Quiet		8	0.125	0.05	10	1.5
	WhistleLow_Loud		8	0.125	0.05	10	4.5

Table C-3. A sample of automated detector classification definitions for the tonal vocalizations of cetacean species expected in the area. Automated detectors are capable of triggering on species and signals beyond those targeted.

Species targeted	Automated detector	Frequency (Hz)	Duration (s)	Bandwidth (Hz)	Other parameters
Humpback whale, killer whale	MFMoanHigh MFMoanHigh_HT	500–2500	0.50–5.00	>150	Max. IB=300 Hz, min. f<1500 Hz
Humpback whale, Rice's whale	MFMoanLow MFMoanLow_HT	100–700	0.50–5.00	>50	Max. IB=200 Hz, min. f<450 Hz
Small dolphins	WhistleHigh_Quiet WhistleHigh_Loud	4000–12,000	0.30–5.00	>700	Max. IB=2000 Hz
	WhistleHigh_Suppress	4000–12,000	0.30–5.00	>700	Max. IB=2000 Hz Suppress detections for SPL > 125 dB between 50 and 1000 Hz
Pilot, killer whale	WhistleLow_Quiet WhistleLow_Loud	1000–10,000	0.80–5.00	>300	Max. IB=1000 Hz, min. f<5000 Hz MultiComponent=1, minComponentduration=0.4s, Min_BW=50Hz
	WhistleLow_Suppress	1000–10,000	0.80–5.00	>300	Max. IB=1000 Hz, min. f<5000 Hz MultiComponent=1, minComponentduration=0.4s, Min_BW=50Hz Suppress detections for SPL > 125 dB between 50 and 1000 Hz

f = frequency, IB = instantaneous bandwidth, SR = sweep rate

C.3. Automatic Data Selection for Validation (ADSV)

To standardize the file selection process for the selection of data for manual analysis, we applied our Automated Data Selection for Validation (ADSV) algorithm. Kowarski et al. (2021) details the ADSV algorithm, and Figure C-1 shows a schematic of the process. ADSV computes the distribution of three descriptors that describe the automated detections in the full data set: Diversity (number of automated detectors triggered per file), Counts (number of automated detections per file for each automated detector), and Temporal Distribution (spread of detections for each automated detector across the recording period). The algorithm removes files from the temporary data set that have the least impact on the distribution of the three descriptors in the full data set. Files are removed until a predetermined data set size (*N*) is reached, at which point the temporary data set becomes the subset to be manually reviewed.

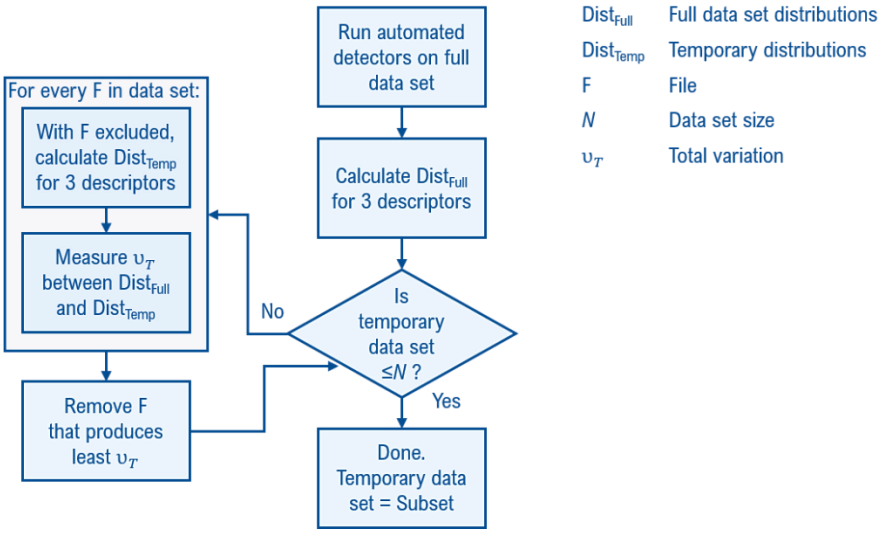

Figure C-5. The Automated Data Selection for Validation (ADSV) process. (source: based on Figure 1 in Kowarski et al. (2021)).

For the present work, an *N* of 0.8 % was selected, largely due to limited scope for this project and marine mammal analysis. Even with limited manual review, the results presented here can be considered reliable, but some caveats should be considered. It is important to note that with such limited data manually reviewed, very rare species may have been missed or their occurrence underestimated. If the 0.8 % subset of data manually analyzed was not sufficiently large to capture the full range of acoustic environments in the full data set, the resulting automated detector performance metrics may be inaccurate and therefore should be taken as an estimate.

C.4. Automated Detector Performance Calculation and Optimization

All files selected for manual validation were reviewed by one of two experienced analysts using JASCO's PAMlab software to determine the presence or absence of every species, regardless of whether a species was automatically detected in the 10 min file. Although the automated detectors classify specific signals, we validated the presence/absence of species at the file level, not the detection level. Acoustic signals were only assigned to a species if the analyst was confident in their assessment. When unsure, analysts would consult one another, peer reviewed literature, and other experts in the field. If certainty could not be reached, the file of concern would be classified as possibly containing the species in question or containing an unknown acoustic signal. Next, the validated results were compared to the automated detector results in three phases to refine the results and ensure they accurately represent the occurrence of each species in the study area.

In Phase 1, the human validated versus automated detector results were plotted as time series and critically reviewed to determine when and where automated detections should be excluded. Questionable detections that overlap with the detection period of other species were scrutinized. By restricting detections spatially and/or temporally where appropriate, we can maximize the reliability of the results. No temporal restrictions were necessary for our automated detector results.

In Phase 2, the performance of the automated detectors was calculated and optimized for each species using a threshold, defined as the number of automated detections per file at and above which detections of species were considered valid.

To determine the performance of each automated detector and any necessary thresholds, the automated and validated results (excluding files where an analyst indicated uncertainty in species occurrence) were fed to a maximum likelihood estimation algorithm that maximizes the probability of detection and minimizes the number of false alarms using the Matthews Correlation Coefficient (MCC):

$$\mathrm{MCC} = \frac{\mathrm{TP} \cdot \mathrm{TN} - \mathrm{FP} \cdot \mathrm{FN}}{\sqrt{(\mathrm{TP} + \mathrm{FP})(\mathrm{TP} + \mathrm{FN})(\mathrm{TN} + \mathrm{FP})(\mathrm{TN} + \mathrm{FN})}}$$

$$P = \frac{\mathrm{TP}}{\mathrm{TP} + \mathrm{FP}}; \quad R = \frac{\mathrm{TP}}{\mathrm{TP} + \mathrm{FN}}$$

where *TP* (true positive) is the number of files in the subset with both manual and automated detections, *FP* (false positive) is the number of files in the subset with automated detections but no manual detections, *FN* (false negatives) is the number of files in the subset with manual detections but no automated detections, and *TN* (true negatives) is the number of files in the subset with neither automated nor manual detections. Automated detector performance was calculated for each species and station.

In Phase 3, detections were further restricted to include only those where *P* was greater than or equal to 0.75. When *P* was less than 0.75, only validated results were used to describe the acoustic occurrence of a species. Dolphin whistles and clicks had automated detectors that performed sufficiently well. Sperm whale clicks were manually detected but not effectively automatically detected, presumably because of the high sound levels at frequencies overlapping with these signals. The occurrence of each species was plotted using JASCO's Ark software as time series showing presence/absence by hour over each day.